Available online at www.sciencedirect.com
ScienceDirect
Geochimica et Cosmochimica Acta 73 (2009) 3337–3358
Geochimica et Cosmochimica Acta
www.elsevier.com/locate/gca

Molecular characterization of dissolved organic matter in pore water of continental shelf sediments

Frauke Schmidt [a,*], Marcus Elvert [a], Boris P. Koch [b], Matthias Witt [c], Kai-Uwe Hinrichs [a]

[a] *MARUM – Center for Marine Environmental Sciences, Leobener Straße, D-28359 Bremen, Germany*
[b] *Alfred Wegener Institute for Polar and Marine Research, Am Handelshafen 12, D-27570 Bremerhaven, Germany*
[c] *Bruker Daltonik GmbH, Fahrenheitstraße 4, 28359 Bremen, Germany*

Received 27 October 2008; accepted in revised form 4 March 2009; available online 19 March 2009

Abstract

Dissolved organic matter (DOM) in sediment pore water is a complex molecular mixture reflecting various sources and biogeochemical processes. In order to constrain those sources and processes, molecular variations of pore water DOM in surface sediments from the NW Iberian shelf were analyzed by ultrahigh-resolution Fourier transform ion cyclotron resonance mass spectrometry (FT-ICR-MS) and compared to river and marine water column DOM. Weighted average molecular element ratios of oxygen to carbon ($(O/C)_{wa}$) and hydrogen to carbon ($(H/C)_{wa}$) provided general information about DOM sources. DOM in local rivers was more oxygenated ($(O/C)_{wa}$ 0.52) and contained less hydrogen ($(H/C)_{wa}$ 1.15) than marine pore water DOM (mean $(O/C)_{wa}$ 0.50, mean $(H/C)_{wa}$ 1.26). The relative abundance of specific compound groups, such as highly oxygenated aromatic compounds or nitrogen-bearing compounds with low H/C ratios, correspond to a high concentration of lignin phenols (160 μg/g sediment dry weight) and a high TOC/TN ratio (13.3) in the sedimentary organic matter and were therefore assigned to terrestrial sources. The lower degree of unsaturation and a higher relative abundance of nitrogen-bearing compounds in the pore water DOM reflected microbial activity within the sediment. One sampling site on the shelf with a high sediment accumulation, and a humic-rich river sample showed a wide range of sulfur compounds in the DOM, accompanied by a higher abundance of lipid biomarkers for sulfate-reducing bacteria, probably indicating early diagenetic sulfurization of organic matter.
© 2009 Elsevier Ltd. All rights reserved.

1. INTRODUCTION

Continental margins are the dominant reservoir of organic matter (OM) burial in the marine environment. In the modern ocean, approximately 90% of the OM is buried along continental margins (Hedges and Keil, 1995). In particular, continental shelves receive a high input of OM derived from different sources. 0.21 Gt C in form of dissolved organic matter (DOM) and 0.17 Gt C in form of particulate organic matter (POM) are annually transported by rivers to the ocean (Ludwig et al., 1996). Besides, the high riverine input of inorganic nutrients fuels the marine primary production on continental shelves. High OM production and short sinking times in shallow water depths are the reason that less OM is remineralized on the shelf and the upper slope. Therefore, around 68% of the marine produced organic carbon is buried in these regions (Hedges and Keil, 1995).

The variety of sources and processes such as sediment remobilization and resuspension due to currents and storm induced bottom waves complicate studying OM preservation in continental shelf sediments. Transport and subsequent deposition cause a mixing of old and fresh OM from various sources and enable increased chemical or biological transformation of OM. Selective adsorption of OM onto mineral surfaces, a process sensitive to changes in

* Corresponding author. Fax: +49 421 21865715.
E-mail address: Frauke.Schmidt@uni-bremen.de (F. Schmidt).

0016-7037/$ - see front matter © 2009 Elsevier Ltd. All rights reserved.
doi:10.1016/j.gca.2009.03.008

chemical conditions (such as salinity and pH, e.g., during the transition river–ocean), can also bias the composition of DOM and POM in the sediment (White et al., 2007; Mead and Goñi, 2008). Both OM pools share common sources and are closely linked by dynamic processes, e.g., dissolution of POM by microbial exoenzymes contributes to DOM (Burdige and Gardner, 1998), whereas DOM flocculates in the course of polymerization (Amon and Benner, 1996; Verdugo et al., 2004). Similar stable carbon isotope ratios of pore water DOM and sedimentary POM emphasize the interlinkage of those processes in marine sediments (Bauer et al., 1995).

DOM in sediment pore waters plays an important role for at least two reasons. On the one hand, it is assumed that pore water DOM is involved in sedimentary preservation of OM (Hedges et al., 1992; Henrichs, 1992; Hedges and Keil, 1995), and on the other hand, it is an important source of nutrients (e.g., Burdige and Zheng, 1998). The integrated dissolved organic carbon (DOC) flux of 0.19 Gt C year^{-1} from coastal and continental margin sediments (Burdige et al., 1999) is comparable to the assumed carbon burial rate of 0.16 Gt C year^{-1} of all marine sediments (Hedges and Keil, 1995). These fluxes suggest that refractory pore water DOM plays an important role in the global oceanic DOM cycle on long terms. Since the nature of the benthic DOM flux (refractory or reactive) is still under debate (Burdige et al., 2002), the identification of specific molecular compounds that serve as markers for sedimentary pore water DOM and their detection in oceanic DOM could be the key to this problem.

One reason for the gap in the knowledge of OM composition and transformation is the analytical challenge to resolve complex molecular mixtures. Thus, 80% of the OM accumulated in sediments cannot be characterized on the molecular level (Hedges et al., 2000). The limitations of DOM analysis are attributed to its high complexity, low concentration and high polarity. Hence, DOM is not amenable to analysis by gas chromatography coupled to mass spectrometry (GC-MS). Other approaches such as pyrolysis or thermochemolysis are invasive methods and can form new products during analysis. NMR spectroscopy, on the other hand, provides an insight into the functionalities of DOM, but due to the complexity of the sample matrix cannot provide in-depth molecular details.

In recent years, the application of Fourier transform ion cyclotron resonance mass spectrometry (FT-ICR-MS) has been applied to the molecular characterization of DOM from different natural environments, e.g., from the marine water column (Koch et al., 2005; Hertkorn et al., 2006; Sleighter and Hatcher, 2008), rivers (Kim et al., 2003), mangrove estuaries (Koch et al., 2005; Tremblay et al., 2007), groundwater (Einsiedl et al., 2007) and soils (Kujawinski et al., 2002a; Kramer et al., 2004; Hockaday et al., 2006). FT-ICR-MS is capable of resolving complex molecular mixtures and provides information about the exact elemental composition of individual compounds. Although analytical challenges such as chemical selectivity during ionization do not allow quantitation, the analytical method of FT-ICR-MS and its data interpretation has been improved over the last years providing a valuable tool for the molecular characterization of low-molecular-weight (LMW) DOM (<1000 Da).

Here, we analyzed for the first time small volumes (50 ml) of marine sediment pore water DOM with FT-ICR-MS from five distinct locations at the shelf and continental slope of the NW Iberian margin. The FT-ICR-MS data were compared to DOM from local rivers which are the major sources of terrestrial material to the shelf (Dias et al., 2002). The associated sedimentary OM was additionally characterized via lipid biomarkers and lignin phenols, which are both routinely used for the identification of OM sources, degradation state and environmental conditions (e.g., Canuel and Martens, 1996; Goñi et al., 2000; Birgel et al., 2004). By this two-pronged approach we specifically aim to identify molecules and compound groups in the sediment pore water DOM that can serve as diagnostic markers for either different OM sources or transformation processes during early diagenesis.

2. MATERIALS AND METHODS

2.1. Sampling site

All samples derive from the Galicia–Minho shelf, the adjacent continental slope and local rivers. The shelf is a storm-dominated, highly energetic environment, located at the NW Iberian margin (Fig. 1). The modern oceanography of Galicia was part of several studies (e.g., Coelho et al., 2002; Oliveira et al., 2002; Vitorino et al., 2002a,b; Alvarez-Salgado et al., 2003). In summer, the northward

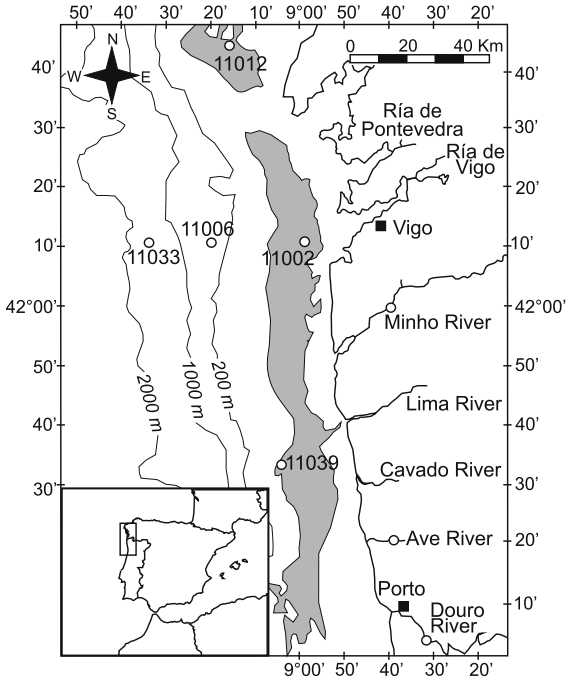

Fig. 1. Sampling sites (GeoB, open circles) at the Galicia–Minho shelf and associated local rivers (distribution of the mid-shelf mudbelt adapted from Dias et al., 2002). Latitude (°N), longitude (°W) and water depth at the sampling sites are listed in Table 1.

flow of the Eastern North Atlantic Central Waters (ENACW) is controlled by trade winds and shifted offshore resulting in upwelling of cold nutrient-rich water masses (Frouin et al., 1990) and an enhanced primary production from March to October. In winter, SW storms produce downwelling conditions resulting in sediment resuspension, remobilization and eventually sediment deposition on the shelf (Jouanneau et al., 2002; Vitorino et al., 2002b) or sediment transport across the shelf break (Dias et al., 2002). Most of the modern sediment accumulates in the mid-shelf mudbelt (Dias et al., 2002). However, sedimentation rates at the Galicia–Minho shelf are difficult to assess due to a sediment mixing layer that comprises the upper 10 cm of sediment at the inner shelf (Jouanneau et al., 2002). The major fraction of sediment at the shelf is supplied by the Douro and Minho River during storms and river floods. Subsequent to the primary sedimentation close to the source, the terrestrial material is remobilized and transported northwards with the predominant currents (Oliveira et al., 2002; Vitorino et al., 2002b).

Due to their importance as sedimentary OM suppliers, Douro and Minho River were sampled to obtain a terrestrial DOM fingerprint. An additional DOM sample was taken from the small Ave River (Fig. 1), which was enriched in humic substances, and serves as a reference site for degraded DOM.

2.2. Sampling

Sampling was performed with a giant box corer in August 2006 during the GALIOMAR expedition (P342) with the German research vessel RV Poseidon at the Galicia–Minho shelf. 50 ml of pore water was extracted with rhizons (Eijkelkamp, pore size 0.1 μm) from each surface sediment sample (depth interval of 0–2 cm). Afterwards, sediments, including additional pore waters, of the same depth horizon were sampled for sedimentary OM analysis (lipids, lignin phenols) and bulk measurements. 50 ml of water from three local rivers were collected and filtered through GF/F filter (Whatman, pore size 0.7 μm). River sampling sites at the local rivers were located at: Douro River 41°06′45 N, 8°32′18 W; Ave River 41°21′06 N, 8°40′54 W; Minho River 42°03′06 N, 8°40′54 W. All water samples were stored in pre-combusted glass bottles without headspace at +4 °C in the dark until further preparation in the home laboratory. Sediment samples were stored in pre-combusted brown glass bottles at −20 °C to avoid OM degradation.

2.3. Dissolved organic matter extraction

Water samples (50 ml) were concentrated by solid-phase extraction on SPE cartridges (PPL bond elute, 200 mg sorbent, suitable for highly polar to nonpolar substances, Varian). Prior to extraction, samples were acidified to pH 2 with hydrochloric acid (HCl, p.a. grade, Merck). After DOM adsorption, the cartridges were rinsed with 6 ml 0.1 M HCl-solution in order to remove any salt from the cartridges, which is a prerequisite for subsequent electrospray ionization (ESI) in FT-ICR-MS analysis. DOM was then eluted with 1 ml methanol (LiChrosolv, Merck) into pre-combusted glass ampoules and stored under nitrogen atmosphere at −18 °C in the dark until analysis.

2.4. Fourier transform ion cyclotron resonance mass spectrometry

Analyses were performed with an Apex Qe mass spectrometer (Bruker Daltonics Inc. Billerica, USA) equipped with a 9.4 T superconducting magnet (Bruker Biospin, Wissembourg, France) and an Apollo II electrospray source. DOM extracts were analyzed in a methanol:water solution (50:50 v/v) with ESI in negative ion mode (capillary voltage: +4 kV) at an infusion flow rate of 2 μl min^{-1}. Spectra were calibrated with arginine clusters and 400–500 scans were added to one spectrum. All ions were singly charged and mass accuracy was below 0.4 ppm. The latter was obtained by internal calibration with compounds, which were repeatedly identified in marine DOM samples (e.g., Koch et al., 2007). For the calculation of molecular formulas, a mass range of 200–600 m/z was selected for peaks with a signal to noise ratio (S/N) of >3. Formula assignment included the elements $^{1}H_{0-\infty}$, $^{12}C_{0-\infty}$, $^{16}O_{0-\infty}$, $^{32}S_{0-2}$, $^{14}N_{0-10}$ and $^{13}C_{0-2}$. A formula tolerance of ±0.5 ppm was considered as a match. The data set was restricted to a molecular element ratio of O/C $\leqslant$ 1.2 and to integer double bond equivalent (DBE) values. DBE defines the number of double bonds and/or rings in a molecule and it is calculated from the number of atoms (N_i) and the valence (V_i) of each element (i) after the following equation:

$$\mathrm{DBE} = 1 + \frac{\sum_i^{i\,\max} N_i(V_i - 2)}{2} \quad (1)$$

For the final dataset we focused on ions with a relative abundance >2% (corresponding to a S/N ratio > 20 in the spectra with the highest intensities (GeoB 11002 and 11006), the most abundant sample compound was set to 100%), using following restrictions with respect to the molecular composition: $^{1}H_{0-\infty}$, $^{12}C_{0-\infty}$, $^{16}O_{0-\infty}$, $^{32}S_{0-2}$, $^{14}N_{0-2}$. With this approach, one unequivocal molecular formula was assigned for each peak in the mass range of 200–500 m/z. Multiple formula matches in the mass range 500–600 m/z were excluded by the homologous series/building block approach (see Koch et al., 2007 for a summary).

Weighted average double bond equivalents (DBE_{wa}), molecular element ratios (e.g., $(O/C)_{wa}$, $(H/C)_{wa}$, $(C/N)_{wa}$) and molecular weight ($(m/z)_{wa}$) were calculated for each sample from the intensity (Int) of each assigned peak (x) using Eq. (2):

$$(\mathrm{O/C})_{\mathrm{wa}} = \frac{\sum(\mathrm{O/C})_x * \mathrm{Int}_x)}{\sum \mathrm{Int}} \quad (2)$$

Aromatic compounds were identified using the modified aromaticity index AI_{mod} (Koch and Dittmar, 2006) after Eq. (3):

$$\mathrm{AI_{mod}} = \frac{1 + \mathrm{C} - 0.5\mathrm{O} - \mathrm{S} - 0.5\mathrm{H}}{\mathrm{C} - 0.5\mathrm{O} - \mathrm{S} - \mathrm{N}} \quad (3)$$

2.5. Dissolved organic carbon and total dissolved nitrogen

To determine the DOC concentration (excluding MeOH) and total dissolved nitrogen (TDN) in the solid-phase extract, an aliquot of the extract was dried with N_2 at room temperature, redissolved in ultrapure water and measured with high-temperature catalytic oxidation using a Shimadzu TOC/TN analyzer equipped with an infrared and a chemiluminescence detector (gas flow oxygen: 0.6 L min^{-1}). In the autosampler, 6 ml of sample volume in pre-combusted vials were acidified with 0.12 ml HCl (2 M) and sparged with oxygen to remove inorganic carbon. 50 μL sample volume was directly injected on the catalyst (heated to 680 °C). Final DOC concentrations were average values of triplicate measurements. Detection limit (5σ of the blank) was 7 μM C with an accuracy of ±2 μM C determined with low carbon water and seawater reference material (DOC-CRM, Hansell Research Lab, University of Miami, US). Due to the limited availability of pore water samples the extraction efficiency could only be exemplary determined for one sample which was available in a larger volume (sample GeoB 11033). The DOC concentration in the redissolved methanol extract was divided by the concentration factor (50) and the DOC concentration in the pore water sample. With this approach we determined an extraction yield of 53% of the total DOC (305 μM DOC) in that sample. Generally, the described method extracts 43–65% of the pelagic DOC (Dittmar et al., 2008).

2.6. Total organic carbon, total nitrogen and total sulfur

Total organic carbon (TOC), total nitrogen (TN) and total sulfur (TS) concentrations were analyzed from the freeze-dried homogenized sediment. TS and TOC was measured with a Leco CS 200. Prior to TOC measurement, the samples were treated with 12.5% hydrochloric acid to remove carbonates. For the TN and TC analysis, 25 mg of the sample was packed in tin boats and measured on a Vario EL III Elemental Analyzer.

2.7. Lipid extraction

Lipid biomarkers were extracted three-times from 30 g of freeze-dried homogenized sediment with a solvent mixture of DCM:methanol (2:1 v/v) with a microwave extraction system (MARS X, CEM) at 80 °C. Prior to extraction, an internal standard mix consisting of 5α-cholestane, behenic acid methylester, 1-nonadecanol and 2-methyloctadecanoic acid was added. The combined extracts were washed with 0.05 M potassium chloride. Water was removed from the organic phase with sodium sulfate and the solvent was evaporated under a stream of nitrogen. Subsequently, the total lipid extract was separated into a hexane-soluble (maltene) and -insoluble (asphaltene) fraction. The maltene fraction was further separated on SPE cartridges (Supelco LC-NH_2, 500 mg sorbent) into four fractions (hydrocarbons, esters and ketones, alcohols, and free fatty acids, Fig. 2) according to the protocol by Hinrichs et al. (2000). Prior to analysis, alcohols were derivatized with bis-(trimethylsilyl)trifluoroacetamide (BSTFA, Merck) in pyridine and analyzed as trimethylsilyl-(TMS)-derivatives; fatty acids were reacted with 12% boron trifluoride in methanol (Merck) yielding fatty acid methylesters. Both reactions were conducted at 70 °C for 1 h. Afterwards, solvent and reagent were removed under a stream of nitrogen and the fractions were stored until analysis at −20 °C in the dark.

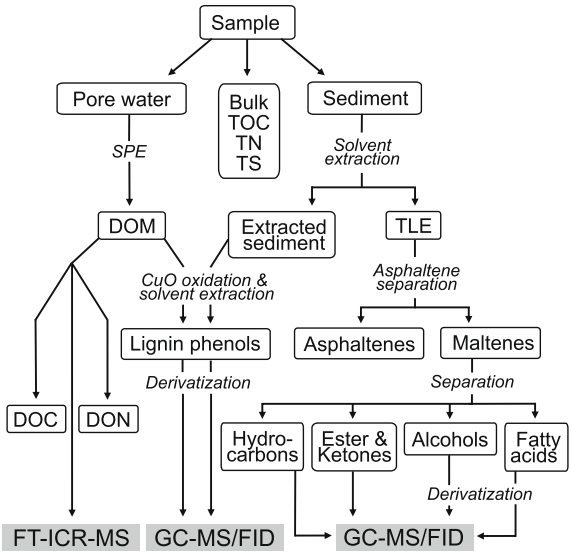

Fig. 2. Scheme of analytical methods applied in this study. Bulk parameters comprise dissolved organic matter (DOM) and particulate organic matter (POM). At each sampling location, DOM was separated by solid-phase extraction (SPE) from pore or river water; lipid biomarkers and lignin phenols were analyzed in the sedimentary OM.

2.8. Lignin extraction

The extraction protocol was adapted from (Hedges and Ertel, 1982). Briefly, 1–2 g of already extracted sediment was oxidized in a microwave vessel under oxygen-free conditions using CuO. Prior to the reaction, 100 mg ammonium-iron(II) sulfate hexahydrate ($Fe_2(NH_4)_2(SO_4) \cdot H_2O$, p.a. Fluka), 1 g DCM extracted CuO powder, and 8 ml of nitrogen-purged sodium hydroxide (p.a. grade, Merck) were added to the sediment under N-atmosphere. The reaction was conducted in a sealed extraction vessel in MARS X at 150 °C for 3 h. After the reaction was completed, an internal standard mixture (ethylvanillin, *t*-cinnamic acid) was added and the sediment was sonicated three-times with 15 ml 1 M sodium hydroxide. The solid and the liquid phase were separated by centrifugation and the combined extracts were acidified with hydrochloric acid to pH 1. Phenols were extracted from the aqueous solution three-times with distilled diethylether, which was treated with $Fe_2(NH_4)_2(SO_4) * H_2O$ in aqueous solution a priori. The extract was dried with sodium sulfate and the solvent was removed under a stream of nitrogen. Phenols were reacted prior to analysis to TMS derivatives using BSTFA in pyridine.

2.9. Gas chromatography coupled to mass spectrometry or flame ionization detection

All four lipid fractions and the phenol extract were analyzed by GC either coupled to a MS or connected to a flame ionization detector (FID). The GC (Thermo Electron Trace GC) was equipped with a 30-m Rtx-5MS fused silica capillary column (0.25 mm i.d., 0.25 μm film thickness) and helium was used as carrier gas (flow rate 1 ml min^{-1}). The lipid extracts were injected in hexane using an injection temperature of 60 °C, a temperature ramp of 10 °C min^{-1} until 150 °C, a temperature ramp of 4 °C min^{-1} and a final temperature of 320 °C (hold time: 30 min). The lignin phenol extract was injected in pyridine:BSTFA (4:1 v/v) in order to keep all carboxylic groups as trimethylsilyl derivatives. The initial temperature of 100 °C was followed by a temperature ramp of 4 °C min^{-1} and a final temperature of 310 °C (hold 12 min). All components were identified via their mass spectrum and quantified by their peak area in the FID chromatogram.

3. RESULTS AND DISCUSSION

3.1. Characterization of sedimentary organic matter

The TOC concentrations in the sediment indicated an OM accumulation in the mudbelt and at the continental slope, whereas the outer shelf sediment received only minor amounts of TOC, indicating a by-passing of material in this area (Table 1). Within the mudbelt, the southernmost sediment sample contained the highest amount of TOC and a high TOC/TN ratio of 13.3. TOC/TN is widely used to determine the proportion of OM from terrestrial and marine sources. The elemental composition of marine phytoplankton is characterized by the Redfield ratio (TOC:N:P 106:16:1, Redfield, 1934, 1958) with a TOC/TN value of 6.7, whereas TOC/TN in vascular plants ranges between 20 and 400 (Hedges et al., 1986). An elevated TOC/TN ratio of 13.3 in the southern mudbelt implied that these sediments received the highest input of terrestrial plant material and emphasized the importance of the Douro River, which has been identified as the major terrestrial OM source at the Galicia–Minho shelf (Dias et al., 2002). The TOC/TN ratio decreased in our study area in northern direction and offshore (Table 1), corresponding to a loss of terrestrial material along the main transport pathways at the shelf. TOC/TN ratios of ca. 7.5 suggested a TOC composition dominated by marine algae and sedimentary microbes. As a fraction of the bulk sediment data, DOC_{SPE} and TDN_{SPE} were measured solely in the extracts of the sediment pore waters. The DOC_{SPE}/TDN_{SPE} ratio reflects similar trends as the TOC/TN data, but in comparison to the bulk sediment the pore water was always enriched in carbon. Similar results were observed in DOM and POM of the marine water column (Hopkinson et al., 1998) and can be explained by a preferential remineralization of easily accessible, fresh DON by microorganisms.

3.2. Spatial distribution of lignin phenols and lipid biomarkers in the particulate organic matter

Lignin is a major compound in vascular land plants and its phenol moieties can be used to trace riverine input of terrestrial material in marine systems (e.g., Ertel and Hedges, 1984; Prahl et al., 1994; Goñi and Hedges, 1995; Goñi et al., 2000). The sum of all detected lignin phenols (vanillin, acetovanillone, vanillic acid, syringealdehyde, acetosyringone, syringic acid, *p*-coumaric acid, ferulic acid) in the sedimentary OM is denoted as ΣLig (Table 2) and resembled the TOC/TN ratio. Accordingly, high concentrations of lignin phenols in the southern mudbelt (Fig. 3b) indicated the accumulation of terrestrial OM. The lignin phenol concentration of 160 μg/g sediment dry weight (dw) is 40-times higher than in the sediment of the continental slope, reflecting a loss of vascular plant material along the transport pathways to the north and offshore.

The relative proportion of specific lignin phenols in the sediment can provide information on the degradation state of lignin (Ertel and Hedges, 1985). Side-chain oxidation, demethylation and aromatic ring cleavage are the major processes during biodegradation of lignin (Tien and Kirk, 1983; Hedges et al., 1988). Propyl-side chain oxidation by white-rot fungi in terrestrial systems results in an increase in acidic CuO reaction products, whereas subaqueous microbial degradation is mainly reflected in a decrease of syringyl and vanillyl phenols due to demethylation reactions (Opsahl and Benner, 1995). The acid to aldehyde ratio of vanillyl (i.e., vanillic acid to vanillin, $(Ad/Al)_V$) indicates terrestrial lignin degradation, if $(Ad/Al)_V$ values are greater than 0.4 (Goñi et al., 1993). At the Galicia–Minho shelf, the $(Ad/Al)_V$ ratio increased from values below 0.4 in the mudbelt sediments to 0.62 and 0.93 in the sediments of the outer shelf and the continental slope, respectively. This increase coincided with the decrease of the total lignin phenols in the sediments (Fig. 3d) along the main transport trajectory, indicating enhanced subaqueous lignin alteration and at the same time a preferential transport or preservation of predegraded terrestrial OM.

Table 1
Location and water depth of all marine sampling sites in this study. Content of total organic carbon (TOC), total nitrogen (TN) and total sulfur (TS) in %, and their ratios (TOC/TN, TOC/TS) analyzed in the bulk sediment from the Galicia–Minho shelf.

Station GeoB	Depth	Longitude (°N)	Latitude (°W)	TOC	TN	TOC/TN	TS	TOC/TS
11039 (mudbelt)	99	41°33′04	9°04′40	2.21	0.17	13.3	0.28	7.89
11002 (mudbelt)	112	42°09′60	8°59′24	0.91	0.11	8.2	0.14	6.50
11012 (mudbelt)	119	42°42′31	9°15′58	0.73	0.11	7.0	0.16	4.56
11006 (outer shelf)	235	42°10′00	9°20′01	0.26	0.03	7.6	0.09	2.89
11033 (continental slope)	1873	42°10′11	9°33′50	1.10	0.15	7.2	0.20	5.50

Table 2
Total lignin abundance (ΣLig) and representative lipid biomarkers (in μg/g dw) in the sediment. The acid to aldehyde ratio of the vanillyl phenols ($(Ad/Al)_V$) was calculated from the total concentration of vanillic acid to vanillin. The Σterr/Σster ratio indicates the relative contributions of terrestrial biomarkers (Σterr including *n*-alkanes (odd numbered C_{25}–C_{35}), *n*-alcohols (even numbered C_{22}–C_{30}) and *n*-fatty acids (even numbered C_{22}–C_{30})) and marine sterol markers (Σster including cholesterol, brassicasterol, and dinosterol) in the sediment. C_{14} to C_{19} mono-*O*-alkyl glycerol ethers (ΣMAGEs) as well as iso- and anteiso C_{15}-fatty acids (*i*- + *ai*-C_{15}FA) derive from autochthonous sulfate-reducing bacteria.

Station GeoB	ΣLig	$(Ad/Al)_V$	*n*-Alkanes	*n*-Alcohols	*n*-Fatty acids	Σterr	Cholesterol	Brassicasterol	Dinosterol	Σster	Σterr/Σster	ΣMAGEs	*i*- + *ai*-C_{15}FA
11039 (mudbelt)	159.9	0.34	2.6	4.8	3.9	11.3	2.5	2.7	2.0	7.2	1.6	3.4	0.6
11002 (mudbelt)	49.6	0.08	1.7	2.7	2.1	6.5	2.4	1.7	1.3	5.4	1.2	3.1	0.5
11012 (mudbelt)	33.6	0.41	1.8	3.5	2.4	7.7	2.4	1.8	1.3	5.5	1.4	3.0	0.3
11006 (outer shelf)	9.9	0.62	0.9	1.9	2.5	5.3	0.9	0.8	0.7	2.4	2.2	0.3	0.3
11033 (continental slope)	4.2	0.93	1.4	1.9	1.4	4.7	0.8	0.6	0.4	1.9	2.5	0.4	0.3

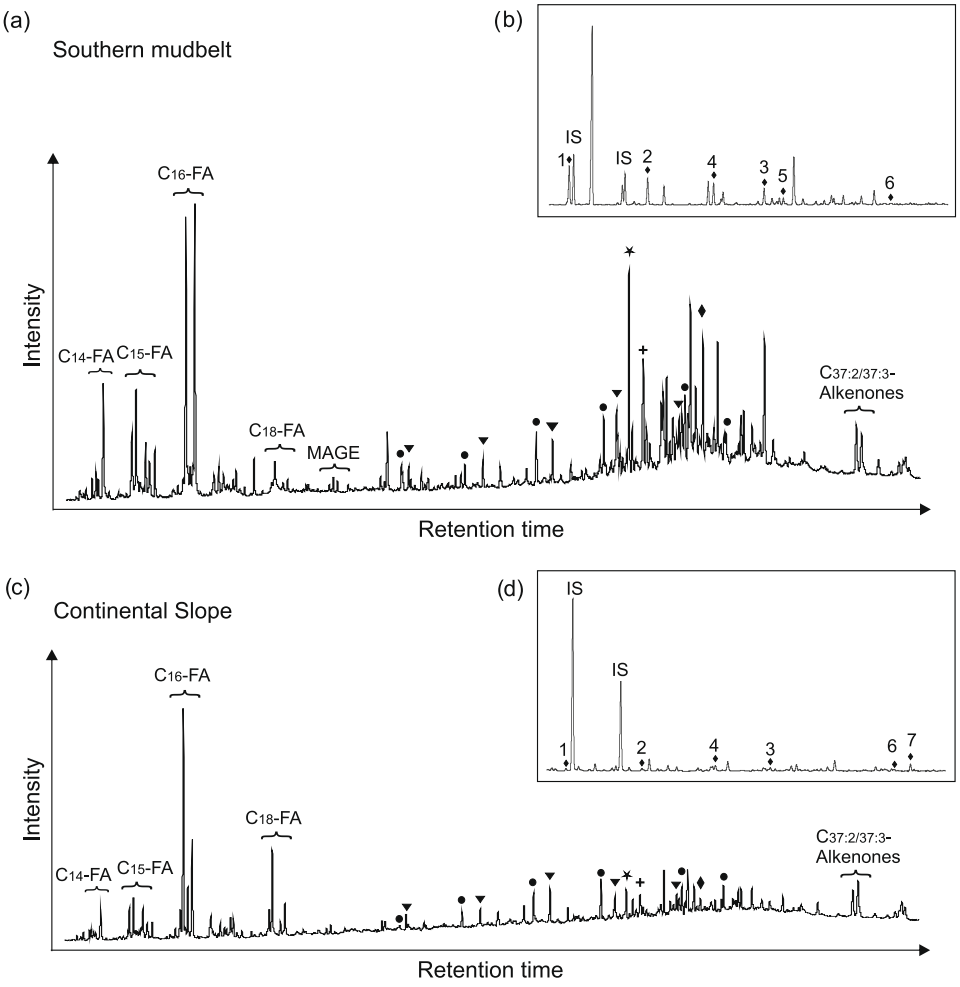

Fig. 3. Gas chromatograms (FID) of the maltene (a and c) and lignin fractions (b and d) of samples from the southern mudbelt (GeoB 11039; a, b) and the continental slope (GeoB 11033; c and d). FA – unsaturated and saturated fatty acids, MAGE – mono-O-alkyl glycerol ethers (C_{14}–C_{19}), circle – *n*-alkanes (C_{25}–C_{35}), triangle – *n*-alcohols (C_{22}–C_{30}), black star – cholesterol, cross – brassicasterol, rhomb – dinosterol. IS – internal standard, 1 – vanillin, 2 – acetovanillone, 3 – vanillic acid, 4 – syringaldehyd, 5 – acetosyringone, 6 – syringic acid, 7 – *p*-coumaric acid.

Lipid biomarkers can also be used to identify sources of OM in the sediment (e.g., Mccallister et al., 2006; Medeiros and Simoneit, 2008; Volkman et al., 2008; Waterson and Canuel, 2008; Yoshinaga et al., 2008). The lipid biomarker

distribution, however, showed a slightly different picture than the lignin phenol and TOC/TN data at the Galicia–Minho shelf. Table 2 lists the absolute abundance of representative lipids at the Galicia–Minho shelf. Long-chain *n*-alkanes with an odd over even carbon number predominance and even numbered long-chain *n*-alcohols and *n*-fatty acids are commonly used as terrestrial biomarkers due to their high abundance in leaf waxes of vascular plants (Eglinton and Hamilton, 1967). For all of these biomarkers, enhanced concentrations were observed in the mudbelt sediments, in particular in the southern mudbelt, which is consistent with the lignin phenol and TOC/TN data. Concentrations of terrestrial markers decreased in the outer shelf and continental slope sediments, but their relative proportions to marine phytoplankton-derived biomarkers such as brassicasterol or dinosterol increased. Together with the low amounts of lignin found here, the lipid biomarker pattern indicates a different transport behavior of single OM fractions, i.e., transport of lignin-containing terrestrial material seems to be restricted in South–North direction, whereas *n*-alkanes, *n*-alcohols and *n*-fatty acids bypass the outer shelf and are also deposited offshore.

3.3. Molecular variations in dissolved organic matter

3.3.1. Dissolved organic matter characterization via molar H/C and O/C ratios

A representative FT-ICR mass spectrum of marine sediment pore water DOM is shown in Fig. 4a. All spectra showed a similar pattern with a slight shift to higher *m/z* in the river water spectra (Table 3). We observed typical mass spacing patterns such as 14.0156 Da for CH_2-groups and an increase of 36.4 mDa for the replacement of O by CH_4, as well as a strong predominance of odd over even mass ions as described elsewhere for various other humic-rich DOM samples (Kujawinski et al., 2002a,b; Stenson et al., 2003; Kramer et al., 2004; Koch et al., 2005). An exception was observed for the Ave River spectrum, which was very distinct from all other samples (Fig. 4c). The spectrum was less intense and the peak intensities were more evenly distributed in the range between 230 and 580 Da, whereas the peaks in the mass spectra of the pore water and other river waters were normally distributed with a maximum in the range of 420–450 Da. An expanded section at the nominal mass 407 of the Ave River DOM spectrum revealed a trend to higher relative intensity of lower masses at each nominal mass (relative intensity maximum: $C_{19}H_{29}O_{10}$, Fig. 4d) compared to the pore water DOM (relative intensity maximum: $C_{20}H_{24}O_9$; Fig 4b). Douro and Minho River spectra showed even higher peak intensities at lower masses. This shift is produced by the higher mass defect of ^1H (1.0078) than of ^{16}O (15.9949) and therefore, it reflects a higher relative O content and/or a lower relative H content in the river DOM (Koch et al., 2008). In total, we identified between 2146 and 2693 unequivocal molecular formulas per sample in the three river DOM samples (Table 3). In the marine pore waters the number of identified molecular formulas was significantly lower and showed the highest number of 2020 molecular formulas in DOM from the southern mudbelt, the sample most strongly influenced by terrestrial input. The decrease in molecular complexity during the coastal export is consistent with other studies (Koch et al., 2005).

A widely used tool for the visualization of compositional variations from FT-ICR-MS data is the van Krevelen diagram (e.g., Kim et al., 2003, 2004, 2006; Kujawinski et al., 2004; Wu et al., 2004; Koch et al., 2005) in which individual

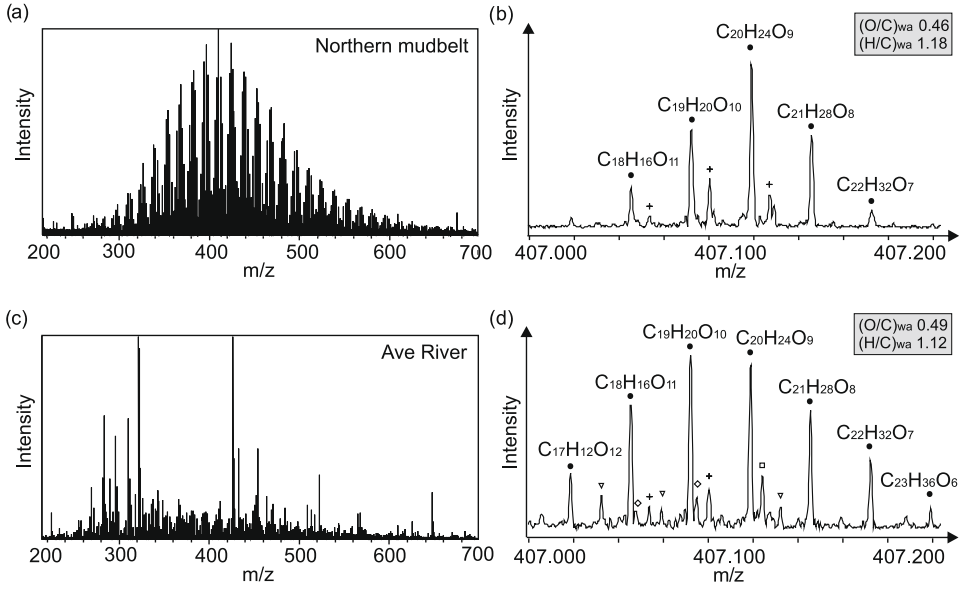

Fig. 4. ESI negative FT-ICR mass spectra and expanded sections of mass spectra at nominal mass 407 of: (a and b) northern mudbelt-derived sediment pore water DOM (GeoB 11012) and (c and d) Ave River DOM. Open rhomb – $C_{13}H_{28}O_{10}S_2$, open square – $C_{26}H_{19}O_3N_2$; following symbols refer to series that are characterized by the replacement of O by CH_4: filled circles – CHO-series from $C_{17}H_{12}O_{12}$ to $C_{23}H_{36}O_6$, cross – nitrogen-bearing series from $C_{17}H_{16}O_{10}N_2$ to $C_{19}H_{24}O_8N_2$, open triangle – sulfur-bearing series from $C_{18}H_{16}O_9S$ to $C_{21}H_{28}O_6S$. $(O/C)_{wa}$ and $(H/C)_{wa}$ refer to CHO-compounds in the presented mass range and reflect a lower relative O content and a higher relative H content in the pore water DOM.

Table 3
Characteristic parameters of pore water and river DOM as well as the contents (in μM) of SPE-extracted dissolved organic carbon (DOC_{SPE}) and total dissolved nitrogen (TDN_{SPE}). Displayed are carbon to nitrogen ratios in the extract (DOC_{SPE}/TDN_{SPE}), numbers of identified molecular formulas (n_{Ion}), the intensity weighted average values of the molecular weight ($(m/z)_{wa}$), double bond equivalents (DBE_{wa}), molar oxygen to carbon ($(O/C)_{wa}$) and hydrogen to carbon ratios ($(H/C)_{wa}$), number of carbon (C_{wa}), nitrogen (N_{wa}) and sulfur atoms (S_{wa}).

Station GeoB	DOC_{SPE}	TDN_{SPE}	DOC_{SPE}/TDN_{SPE}	n_{Ion}	$(m/z)_{wa}$	DBE_{wa}	$(O/C)_{wa}$	$(H/C)_{wa}$	C_{wa}	N_{wa}	S_{wa}
11039 (mudbelt)	153	10	15	2020	421.08	8.61	0.52	1.26	19.48	0.32	0.09
11002 (mudbelt)	94	4*	26*	1980	411.99	8.40	0.50	1.26	19.24	0.37	0.02
11012 (mudbelt)	189	15	13	1418	430.44	8.91	0.51	1.24	20.15	0.34	0.03
11006 (outer shelf)	270	12	23	1780	426.92	8.95	0.50	1.24	20.09	0.35	0.02
11033 (continental slope)	189	16	12	1858	422.63	8.63	0.49	1.29	19.85	0.61	0.01
Douro River	150	8*	20*	2146	444.31	9.55	0.52	1.18	20.66	0.20	0.03
Minho River	107	6*	17*	2211	449.57	10.18	0.52	1.13	21.02	0.16	0.02
Ave River	209	22	11	2694	401.88	8.92	0.49	1.19	18.81	0.16	0.30
Atlantic deep water	–	–	–	624	453.03	9.14	0.50	1.24	21.34	0.11	–

* TDN_{SPE} close to the limit of quantitation.

molecular formulas are plotted on the basis of their molar H/C and O/C ratios. Thus, each dot in the diagram represents one or more molecular formulas with a specific O/C and H/C ratio. The pattern in the van Krevelen diagram can reflect the sources of DOM but also reaction pathways (Kim et al., 2003), e.g., enzymatic hydroxylation by microbes or photodegradation. Fig. 5 compares changes of DOM along the main transport route from the Douro River across the shelf system (central mudbelt – outer shelf – continental slope). Distinct features were revealed among the different samples such as specific molecular formulas at low O/C and high H/C values in the marine sediment pore waters as well as molecular formulas at low H/C and intermediate O/C values, which were only present in the river DOM. In general, the composition of sediment pore water DOM was gradually shifted in the van Krevelen diagram to higher H/C and lower O/C ratios along the transport pathway and $(O/C)_{wa}$ and $(H/C)_{wa}$ ratios of pore water DOM were similar to those of DOM from the marine water column (Atlantic deep water as marine reference sample in Table 3). Similar trends were observed in earlier studies by comparing marine DOM samples with river DOM (Sleighter and Hatcher, 2008) or mangrove pore water DOM (Koch et al., 2005). The variations in the oxygen and hydrogen content of DOM appear to be linked to changes in OM sources. River DOM is more oxygenated and contains less hydrogen, which points to a higher aromaticity in the terrestrial OM due to high contributions of lignins or tannins. The contribution of aliphatic compound types from algal detritus and/or microbial biomass in marine sediment is reflected in lower $(O/C)_{wa}$ and higher $(H/C)_{wa}$ ratios.

A change in $(H/C)_{wa}$ and $(O/C)_{wa}$ ratios may also be explained by biodegradation processes, which have been shown to selectively remove oxygen-rich molecules from DOM (Kim et al., 2006). This is probably the case for Ave River DOM with a typical terrestrial $(H/C)_{wa}$ ratio of 1.19 and a low $(O/C)_{wa}$ ratio of 0.49, i.e., the latter being similar to marine Atlantic deep water DOM.

Referring to the peak heights in the spectra, the most abundant compounds in all samples were located in the center of the van Krevelen diagram (O/C 0.5–0.8, H/C 1.0–1.5), correlating with O/C and H/C ratios of lignins and tannins (Fig. 5). However, in a recent study by Lam and coworkers (2007) no lignin methoxy groups were detected by NMR spectroscopy in Lake Ontario DOM. 8% of the carbon in Lake Ontario DOM was associated with aromatics, 17% with carbohydrates and the remaining 75% with terpenoid derived material (linear and alicyclic terpenoids). One particular compound group belonging to the latter fraction comprises carboxylic-rich alicyclic molecules (CRAM, molecules with a cyclic backbone and a high degree of carboxylation), previously identified as major compounds in deep ocean DOM (Hertkorn et al., 2006). Several molecular formulas that are assigned to CRAM were present in all DOM samples from Galicia (e.g., $C_{28}H_{32}O_{13}$, corresponding to a mass of 576.546 Da). However, the samples contained also molecular formulas of degraded lignin (e.g., $C_{27}H_{28}O_{12}$, see Stenson et al., 2003) and especially in river DOM and the pore water DOM from the southern mudbelt lignin contributions are very likely, since high lignin phenol concentrations were detected in the sedimentary OM.

Fig. 6 shows the molecular differences between the samples in a cluster diagram. The cluster analysis was carried out on the basis of all identified molecular formulas and the relative intensity of the referring ion in the spectrum. By this, weighted average element ratios, molecular weight distribution, etc. are directly reflected in the degree of similarity between the samples, e.g., the exceptional position of the Ave River was supported in the lowest degree of similarity compared to all other samples. Douro and Minho River grouped together ($S = 84$), well separated from the pore water samples. Within the marine samples the pore water DOM from the continental slope differed with $S \leqslant 0.72$.

3.3.2. Dissolved organic matter characterization via molecular mass and DBE

DOM from the three environments, i.e., sediment pore water, river, and Atlantic deep water, differed significantly regarding their $(m/z)_{wa}$ and DBE_{wa} (Table 3). The $(m/z)_{wa}$

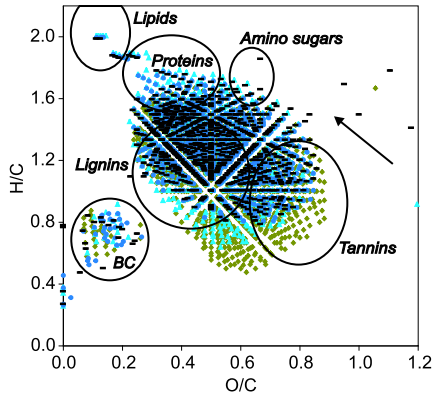

Fig. 5. van Krevelen diagram of CHO-formulas in DOM from the Galicia–Minho shelf. A shift in direction of the arrow is observed to higher H/C and lower O/C ratios from the Douro River (green rhombs) to the central mudbelt (GeoB 11002, light blue triangles) down to the outer shelf (GeoB 11006, blue circles) and the continental slope (GeoB 11033, black dashes). Black circles correspond to general compound classes (adapted from Kim et al., 2003; Sleighter and Hatcher, 2008) and are indicated for reference, not necessarily implying the presence of these compounds in the DOM samples.

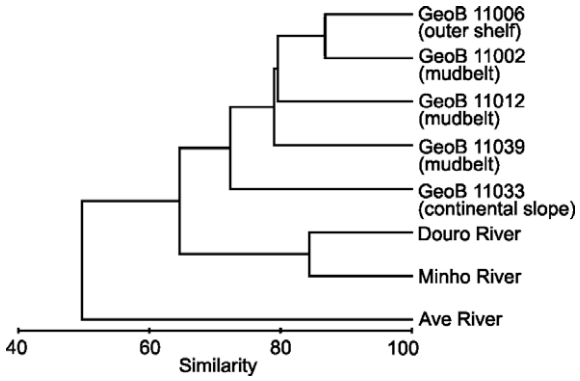

Fig. 6. Cluster analysis (Bray Curtis Similarity) based on all identified molecular formulas having a relative intensity $\geqslant 2\%$. Cluster analyses visualize similarities/dissimilarities between samples based on a multidimensional data set. The x-axis represents the degree of similarity; the vertical lines of the branches indicate the similarity value. A similarity value of $S = 100$ would mean that all molecular formulas in the samples are identical.

in marine pore water DOM ranged from 411.99 to 430.34, which is much lower compared to the Atlantic deep water ($(m/z)_{wa}$ 453.03) and the river DOM ($(m/z)_{wa}$ 444.27 and 449.57 for Douro and Minho River, respectively).

In the sediment pore water, lower $(m/z)_{wa}$ was correlated with lower DBE_{wa}. The loss of aromatic molecules and molecules with high molecular weight (low DBE_{wa} and $(m/z)_{wa}$, respectively) was observed previously by Tremblay et al. (2007) who compared mangrove pore water and water column DOM in a Brazilian estuary. These authors explained this loss with photodegradation that took place during transport of DOM in the water column. At the Galicia–Minho shelf, a shift to lower DBE_{wa} and $(m/z)_{wa}$ from river water to sediment pore water suggested that in situ transformation processes are taking place. Sediment pore water DOM is a heterogeneous mixture of organic compounds including large molecules, e.g., proteins, humic substances, and smaller molecules, e.g., amino acids and short-chain organic acids (e.g., Henrichs, 1992). The DOC concentration in marine pore water is usually up to a magnitude higher than in the surrounding bottom water, implying net production of DOM in the sediment as a result of remineralization (Burdige et al., 2002). Intermediates during remineralization processes such as hydrolysis and fermentation produce smaller molecules and LMW-DOM, thus reducing $(m/z)_{wa}$, which is consistent with the trends observed in our study. Besides, the highly degraded DOM in the Ave River (see also Section 3.3.5) had by far the lowest $(m/z)_{wa}$ and a DBE_{wa} value closely similar to sediment pore water DOM. Furthermore, recent studies with FT-ICR-MS reported a shift to lower m/z in stream DOM (Kim et al., 2006) and fulvic acids (Einsiedl et al., 2007), which were both exposed to microbial activity.

3.3.3. Sources and occurrence of aromatic ring structures

In order to separate aromatic compounds from the bulk FT-ICR-MS dataset, we applied the modified aromaticity index (AI_{mod}, Koch and Dittmar, 2006). This ratio emphasizes the proportion of double bonds in a molecule compared to the total number of carbon atoms in consideration of the presence of heteroatoms such as sulfur and nitrogen. Based on the assumption that the carboxyl group is the dominant oxygen-containing functional group in DOM (Hertkorn et al., 2006; Sleighter and Hatcher, 2008), AI_{mod} considers that 50% of the oxygen is bound with π-bonds as carbonyl oxygen, which would artificially increase the number of DBE in a molecule. In our samples, we distinguished two groups of aromatic structures (Table 4), one with high O/C ratios ($O/C > 0.4$, DBE-O from 2 to 11) and one with low O/C ratios ($O/C < 0.2$, DBE-O from 15 to 32). Both groups comprised CHO-compounds as well as compounds containing heteroatoms (S, N) and will be separately discussed in the following.

3.3.3.1. Aromatic compounds with low O/C ($\leqslant 0.2$). In recent studies, aromatic compounds with low O/C values in DOM samples were assigned to black carbon (BC) (Kim et al., 2004; Kramer et al., 2004). BC, a group of incomplete combustion products of fossil fuels and biomass, is very heterogeneous with respect to its size, age, and chemical composition (Schmidt and Noack, 2000). At the Galicia–Minho shelf, BC was present in all samples and showed no obvious trend in its distribution. The presence of BC in river water DOM can be best explained by the frequent occurrence of wildfires in northern Spain and Portugal. During the time of sampling in August 2006, large parts of North West Iberia were affected by those forest fires, which provide a possible source of BC in the three rivers. Marine sediments can receive BC on several pathways. One is air transport and dry-fall out of combustion products from wildfires or anthropogenic production, another one is river trans-

Table 4
Distributional pattern and source assignments of identified compound classes in river and sediment pore water DOM.

Compound class	Distribution	Potential sources	Previous Reference
CHO-compounds O/C < 0.6 H/C > 1.7	Sediment pore waters	Aliphatic molecules from algal and microbial biomass	Koch et al. (2005) Sleighter and Hatcher (2008)
CHO-compounds O/C > 0.5 H/C < 0.8	Rivers, S'mudbelt, central mudbelt	Terrestrial OM, e.g., fulvic acids	Kim et al. (2003) Stenson et al. (2003) Koch et al. (2005) Sleighter and Hatcher (2008)
CHO-compounds O/C 0.5–0.8 H/C 1.0–1.5	Non specific	CRAM, lignins, tannins	Kim et al. (2003) Hertkorn et al. (2006) Tremblay et al. (2007) Sleighter and Hatcher (2008)
Aromatic compounds O/C ⩽ 0.2	Non specific	Black carbon from soils and wild fires	Kim et al. (2003) Kramer et al. (2004)
Aromatic compounds O/C > 0.4	Rivers, S'mudbelt	Humic acids from soils or modified BC	Kim et al. (2003) Kramer et al. (2004) Hockaday et al. (2006) Dittmar and Koch (2006)
Nitrogen-bearing compounds H/C > 1.5	Continental slope	Degraded proteins from fresh microbial and algal biomass	Kujawinski et al. (2004) Sleighter and Hatcher (2008)
Nitrogen-bearing compounds O/C 0.4–0.8 H/C 0.6–0.8	Rivers, S'mudbelt	Terrestrial compounds	
Sulfur-bearing compounds	Ave River, S'mudbelt	Early diagenetic sulfurization of OM	

port which is promoted by the fairly high resistance to biodegradation (Kim et al., 2004). However, the absence of typical combustion products from wild fires such as 3-methoxyfriedelane, *n*-nonacosan-10-ol or methoxyphenols (see Simoneit, 2002) in the lipid fraction of our samples pointed to a different origin, potentially hydrocarbons from ship fuels. Alternatively, BC-like compounds in the pore water could also have an older age and derive from wild fires in former times. Compared to solvent-extractable combustion products in the sedimentary OM, it is most likely that BC compounds survive during transport from the soil to the sediments due to their very high resistance against degradation.

3.3.3.2. Aromatic compounds with high O/C (>0.4). We detected a high number of aromatic structures with high O/C values in the river DOM as well as in the sediment pore water DOM from the southern mudbelt (Fig. 7). These aromatic compounds were highly abundant in number in the river DOM and decreased gradually in the mudbelt northward along the main transport route and were not detected in the pore water DOM from the northern mudbelt, outer shelf and continental slope. The significant correlation with lignin and *n*-alkanes in the sedimentary OM ($r = 0.9$, for a confidence level $\alpha = 0.05$) suggests a terrestrial origin of those compounds. Aromatic compounds with high O/C values could be derived from microbially mediated oxidation of BC (Dittmar and Koch, 2006), which takes place in soils and sediments. Several microbes are able to metabolize BC via enzymatic reactions and accordingly increase the number of carboxylic, hydroxylated and methoxylated aliphatic groups, which then increases the O/C ratio and generally the water solubility (Rudolphi et al., 1991; Willmann and Fakoussa, 1997; Decesari et al., 2002). In recent studies, carboxylic aromatic ring structures with high oxygen content were detected as major constituents in humic acid leachates of soil charcoal (Hockaday et al., 2006), in volcanic ash soil humic acids (Kramer et al., 2004) and in bog and black water DOM (Kim et al., 2004). Therefore, likely sources of these compounds in river DOM are humic acids, washed out from soil or modified BC compounds. For the occurrence of those compounds in the pore water, two major pathways are conceivable: BC is oxidized in soils, subsequently dissolved, transported via rivers to the ocean, and incorporated into the oceanic DOM pool and ultimately into sediment pore water due to exchange processes with the bottom water. Alternatively, particulate BC, which is

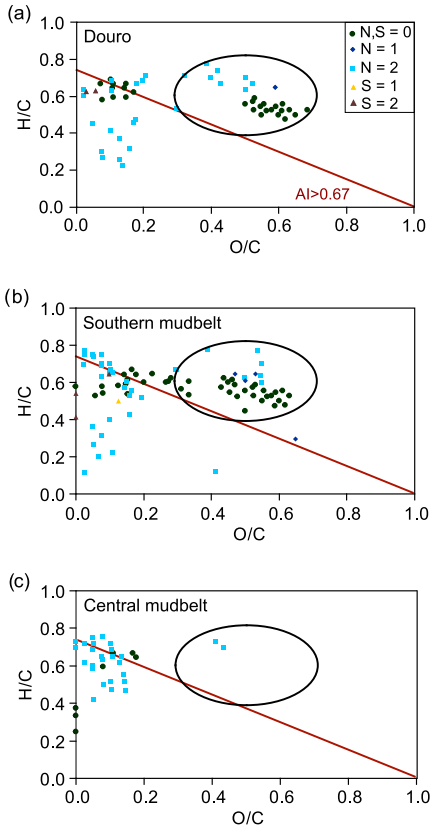

Fig. 7. Detailed van Krevelen diagram of aromatic compounds (modified aromaticity index $AI_{mod} \geqslant 0.67$), including N and S for: (a) the Douro River, (b) the southern (GeoB 11039) and (c) the central mudbelt (GeoB 11002). The non-modified aromaticity index $\geqslant 0.67$ (red line) assigns all condensed aromatics with low oxygen content. Circles mark highly oxygenated aromatics of terrestrial origin.

transported in the POM fraction via rivers or as aerosols via the atmosphere, can be oxidized by microbes in marine sediments, where the products dissolve and accumulate in the pore water DOM.

3.3.4. Spatial variations of nitrogen-bearing compounds

Compounds with molecular formulas including one or two nitrogen atoms were present in all DOM samples in varying relative abundance. The FT-ICR mass spectra revealed a change from low numbers of nitrogen-bearing compounds in the river DOM ($N_{wa} = 0.16$–0.20) to higher amounts in northward direction along the mudbelt ($N_{wa} = 0.32$–0.37) and offshore at the continental slope ($N_{wa} = 0.61$). Similar results of an increase in nitrogen-bearing compounds offshore were detected in a recent study along a river to ocean transect of the Chesapeake Bay (Sleighter and Hatcher, 2008).

The van Krevelen diagram in Fig. 8 reflects the high variety in nitrogen-bearing compounds in the pore water DOM from the continental slope in comparison to Douro River DOM. Striking features are the contributions from compounds with two N-atoms, plotting mainly in regions of the van Krevelen diagram where proteins, oligopeptides, amino sugars and highly aromatic compounds are expected. These compounds were exclusively present in the continental slope DOM. A high relative abundance of nitrogen-bearing compounds, which were concentrated in the protein area of the van Krevelen diagram, was also detected by Kujawinski et al. (2004) who analyzed DOM produced by bacteria and protozoan cultures. Although proteins are not in our analytical window ($200 < m/z < 600$), the occurrence of degradation products and intermediates with lower molecular weight are expected constituents in pore water DOM. The lack of those molecules in the other pore water samples may be related to variations in the exchange between pore water and bottom water at the different sampling locations. Sediment deposits at the Galicia–Minho shelf are subjected to sediment mixing due to strong currents and storm induced bottom waves in winter (Jouanneau et al., 2002; Vitorino et al., 2002b) and therefore, pore water and bottom water are regularly exchanged on a seasonal basis. In contrast, calm sedimentation conditions at the continental slope result in a continuously accumulation of clay-rich sediment. Additionally, diffusion rates of pore water are reduced in clay-rich densely packed sediments (e.g., Tryon et al., 2001; Janssen et al., 2005), enhanc-

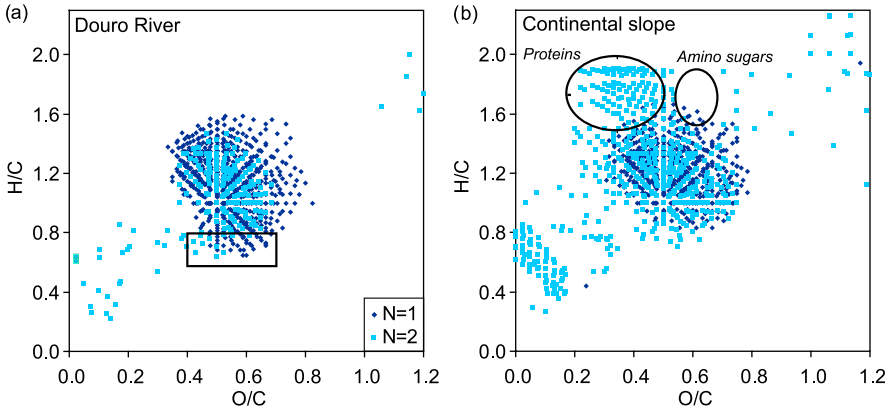

Fig. 8. van Krevelen diagram of nitrogen-bearing molecular formulas in DOM of: (a) the Douro River (rectangle marks compounds of terrestrial origin) and (b) the continental slope (GeoB 11033). Circles correspond to O/C and H/C ratios of proteins and amino sugars (Kim et al., 2003).

ing the preservation of nitrogen compounds in the pore water DOM at the continental slope. Alternatively, this distinct signal in the continental slope pore water DOM may also reflect a different OM quality, e.g., similarly shown in Amazon River POM (e.g., Hedges et al., 1986).

A specific compound group with O/C ratios of 0.4–0.7 and relatively low H/C ratios of 0.6 and 0.8 was observed in the river DOM (rectangle in Fig. 8a). Molecular formulas related to these ratios (e.g., $C_{19}H_{15}O_{11}N$) were also present in the southern mudbelt but missing in all other pore water samples, thus pointing to a terrestrial source of this compound group. Nevertheless, at this point, the knowledge of the occurrence of distinct nitrogen compounds in DOM is still limited and therefore needs further research to understand their distribution and structural diversity.

3.3.5. Sulfur compounds as indicators for early diagenesis?

All DOM samples contained several compounds with one or two sulfur atoms in the formulas. Compounds with higher sulfur (and also nitrogen) content have been omitted, since it was necessary to restrict the number and type of isotopes for the molecular formula calculation in an a priori assumption (Koch et al., 2007).

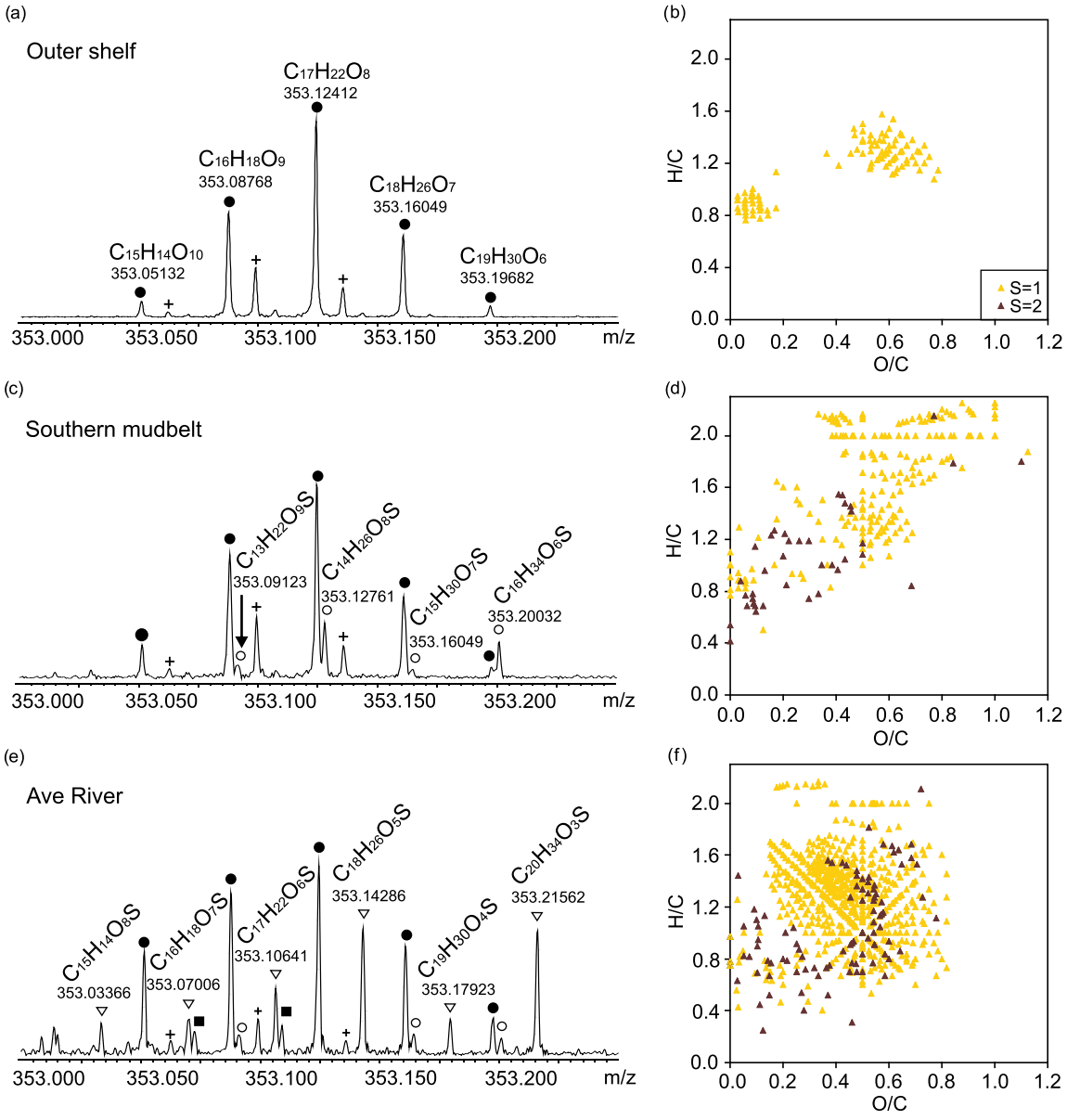

Fig. 9. FT-ICR mass spectra at 353 *m/z* for: (a) the outer shelf (GeoB 11006), (c) the southern mudbelt (GeoB 11039) and (e) the Ave River and van Krevelen diagram of all characterized S-bearing compounds for: (b) the outer shelf (GeoB 11006), (d) the southern mudbelt (GeoB 11039) and (f) the Ave River. Molecular formulas and exact masses refer to filled circles (a), to open circles (b) and to open triangles (c). Cross – nitrogen series, where CH_4 replaces O from $C_{14}H_{14}O_9N_2$ to $C_{16}H_{22}O_7N_2$, filled squares – $C_{12}H_{18}O_{12}$, $C_{13}H_{22}O_{11}$.

In general, the relative abundance of S_{wa} in the FT-ICR-MS data was around 0.02. Intriguing was the high number of sulfur-bearing compounds in the Ave river (S_{wa} 0.30) and in the sediment pore water DOM from the southern mudbelt (S_{wa} 0.09). Exemplary FT-ICR mass spectra at the mass 353 are shown in Fig. 9a, c and e (outer shelf, southern mudbelt and Ave River). The outer shelf represents samples with a S_{wa} value of 0.02 and exhibited no sulfur compounds at the nominal mass 353, whereas the southern mudbelt and the Ave River showed several sulfur formulas, e.g., $C_{16}H_{34}O_6S$. In the spectrum of the Ave River, the sulfur-bearing compounds reached intensities of up to 2/3 relative to CHO-compounds, emphasizing the importance of dissolved organic sulfur compounds in this sample. The van Krevelen diagram of all sulfur formulas in the DOM at the outer shelf revealed two specific compound groups. One group located at 0.4–0.8 O/C and 1.1–1.6 H/C values and the other at 0.0–0.2 O/C and 0.8–1.0 H/C values (Fig. 9b). By contrast, the Ave River and the southern mudbelt sample showed a widespread occurrence of sulfur-bearing compounds in the van Krevelen diagram (Fig. 9d and f). Since none of the observed compounds (e.g., $C_{15}H_{26}O_6S$, $C_{22}H_{34}O_9S_2$) contained nitrogen, a relationship to degradation products of proteins is unlikely. We therefore suggest that early diagenetic sulfurization of organic matter is the primary source of the detected sulfur compounds in the Ave River and the southern mudbelt DOM. Although total sulfur concentrations in the sediment from the Galicia–Minho shelf were low and the TOC/TS values of 2.89–7.89 exceeded the commonly assumed average values for modern shelves of 2.8 (Berner, 1982), the southern mudbelt showed an 3-fold higher TS concentration than the outer shelf. Sulfurization reactions are known to proceed during the early stages of sedimentary diagenesis and have been detected even at the sediment water interface (Sinninghe Damste and De Leeuw, 1990; Wakeham et al., 1995). The southern mudbelt probably provides at least seasonally (summer) anoxic conditions, which are prerequisite for the sulfurization reactions. Furthermore, a range of mono-*O*-alkyl glycerol ethers (C_{14} to C_{19}) and iso/anteiso-$C_{15:0}$ fatty acids, both groups indicative of sulfate-reducing bacteria (Taylor and Parkes, 1983; Rütters et al., 2001), were detected in the sedimentary OM samples of the mudbelt with the highest amounts found at the southernmost sampling site (Table 2 and Fig. 3a). The activity of sulfate-reducing bacteria in these sediments provides hydrogen sulfide and other reduced sulfur species, which could subsequently react with the OM.

The Ave River DOM, however, represents probably older, highly degraded OM, enriched in humic substances. OM at this site had repeatedly passed anoxic conditions in soils or anoxic bottom waters, in which sulfurization processes took place, thus explaining the occurrence and diversity of sulfur-bearing compounds. Further research is needed to elucidate the origin and significance of sulfur-containing DOM.

4. SUMMARY AND CONCLUSIONS

Although FT-ICR-MS delivers extensive molecular data for humic material it must be considered that this method so far is not quantitative. The ionization efficiency might vary strongly between aromatic and more apolar aliphatic compounds. The isolation of single compounds by separation methods or in the ICR cell as well as structure elucidation in fragmentation experiments will be the prerequisite for any quantitative approach and is one of the goals of our future research. Moreover, since the molecular structures of the compounds in this study are not exactly determined, tests with artificial standards cannot be applied so far. The conclusions which were drawn in this study are based on relative peak abundances and allowed a fingerprinting approach for organic matter sources. The observed variations of the molecular DOM composition on the shelf are linked to both source variations and biogeochemical processes in the sediment. Compositional variations in DOM are also reflected in distributions of compounds in the sedimentary OM, i.e., lignin phenols, selected lipid biomarkers, and in elemental compositions of bulk OM. Table 4 summarizes the source assignments of major compound groups detected in pore water DOM and the resulting interpretations. The major observations are:

1. Highly oxygenated aromatic compounds and nitrogen-bearing compounds with H/C 0.6–0.8 are probably derived from terrestrial sources as suggested by their distributional pattern similar to the lignin phenol abundance and TOC/TN ratios in concurrently collected sediment samples.
2. Another nitrogen-bearing compound group with high H/C ratios was dominantly found in continental slope DOM and appears to be indicative for microbial activity in the marine sediment, which was also reflected in the lower number of DBEs.
3. Remarkably high concentrations of sulfur compounds in the southern mudbelt and Ave River DOM probably result from early diagenetic alteration of OM and have not been documented in previous FT-ICR-MS studies.

ACKNOWLEDGMENTS

We thank the crew of R.V. Poseidon, Till Hanebuth and the scientific shipboard party of the GALIOMAR cruise. Further thanks go to Brit Kockisch for support during sampling and the performance of TOC measurements. We acknowledge Hella Buschoff for TN analysis and Xavier Prieto for support in the lab. We are grateful to Rodger Harvey and three anonymous reviewers for their thoughtful comments on the manuscript. Funding was provided by the "Deutsche Forschungsgemeinschaft" through DFG-Research Center / Excellence Cluster "The Ocean in the Earth System" and the Bremen International Graduate School for Marine Sciences (GLOMAR).

APPENDIX A

Identified sum formulas in pore water DOM from the southern mudbelt (GeoB 11039) shown for the mass range from 350 to 400 Da.

Sum formula	Mass	Error (ppm)	O/C	H/C	DBE	AI_{mod}
$C_{15}H_{13}O_9N_1$	350.05165	−0.30	0.60	0.87	10	0.53
$C_{16}H_{17}O_8N_1$	350.08811	−0.09	0.50	1.06	9	0.41
$C_{17}H_{21}O_7N_1$	350.12450	−0.07	0.41	1.24	8	0.32
$C_{18}H_{25}O_6N_1$	350.16099	0.22	0.33	1.39	7	0.25
$C_{15}H_{12}O_{10}$	351.03580	0.08	0.67	0.80	10	0.50
$C_{16}H_{16}O_9$	351.07211	−0.13	0.56	1.00	9	0.39
$C_{15}H_{16}O_8N_2$	351.08334	−0.14	0.53	1.07	9	0.44
$C_{17}H_{20}O_8$	351.10853	−0.03	0.47	1.18	8	0.31
$C_{14}H_{24}O_8S_1$	351.11176	−0.43	0.57	1.71	3	−0.22
$C_{16}H_{20}O_7N_2$	351.11976	−0.04	0.44	1.25	8	0.33
$C_{18}H_{24}O_7$	351.14495	0.07	0.39	1.33	7	0.24
$C_{17}H_{24}O_6N_2$	351.15623	0.20	0.35	1.41	7	0.25
$C_{19}H_{28}O_6$	351.18127	−0.12	0.32	1.47	6	0.19
$C_{15}H_{15}O_9N_1$	352.06739	−0.04	0.60	1.00	9	0.42
$C_{16}H_{19}O_8N_1$	352.10380	0.03	0.50	1.19	8	0.32
$C_{17}H_{23}O_7N_1$	352.14021	0.10	0.41	1.35	7	0.24
$C_{18}H_{27}O_6N_1$	352.17673	0.48	0.33	1.50	6	0.18
$C_{14}H_{10}O_{11}$	353.01496	−0.21	0.79	0.71	10	0.53
$C_{15}H_{14}O_{10}$	353.05135	−0.20	0.67	0.93	9	0.40
$C_{14}H_{14}O_9N_2$	353.06281	0.44	0.64	1.00	9	0.47
$C_{16}H_{18}O_9$	353.08783	0.07	0.56	1.13	8	0.30
$C_{13}H_{22}O_9S_1$	353.09123	0.15	0.69	1.69	3	−0.33
$C_{15}H_{18}O_8N_2$	353.09901	−0.08	0.53	1.20	8	0.33
$C_{17}H_{22}O_8$	353.12420	0.02	0.47	1.29	7	0.23
$C_{14}H_{26}O_8S_1$	353.12761	0.13	0.57	1.86	2	−0.33
$C_{16}H_{22}O_7N_2$	353.13541	−0.04	0.44	1.38	7	0.24
$C_{18}H_{26}O_7$	353.16058	0.01	0.39	1.44	6	0.17
$C_{15}H_{30}O_7S_1$	353.16409	0.40	0.47	2.00	1	−0.33
$C_{16}H_{34}O_6S_1$	353.20036	0.08	0.38	2.13	0	−0.33
$C_{23}H_{46}O_2$	353.34237	−0.38	0.09	2.00	1	0.00
$C_{15}H_{17}O_9N_1$	354.08308	0.07	0.60	1.13	8	0.32
$C_{16}H_{21}O_8N_1$	354.11953	0.25	0.50	1.31	7	0.23
$C_{17}H_{25}O_7N_1$	354.15569	−0.38	0.41	1.47	6	0.16
$C_{14}H_{12}O_{11}$	355.03075	0.18	0.79	0.86	9	0.41
$C_{18}H_{12}O_8$	355.04602	0.22	0.44	0.67	13	0.64
$C_{15}H_{16}O_{10}$	355.06710	0.08	0.67	1.07	8	0.30
$C_{14}H_{16}O_9N_2$	355.07838	0.21	0.64	1.14	8	0.33
$C_{16}H_{20}O_9$	355.10350	0.12	0.56	1.25	7	0.22
$C_{15}H_{20}O_8N_2$	355.11472	0.09	0.53	1.33	7	0.22
$C_{17}H_{24}O_8$	355.13985	0.02	0.47	1.41	6	0.15
$C_{14}H_{28}O_8S_1$	355.14312	−0.26	0.57	2.00	1	−0.44
$C_{16}H_{24}O_7N_2$	355.15103	−0.13	0.44	1.50	6	0.14
$C_{18}H_{28}O_7$	355.17626	0.09	0.39	1.56	5	0.10
$C_{19}H_{32}O_6$	355.21248	−0.37	0.32	1.68	4	0.06
$C_{17}H_{11}O_8N_1$	356.04105	−0.39	0.47	0.65	13	0.71
$C_{14}H_{15}O_{10}N_1$	356.06236	0.11	0.71	1.07	8	0.31
$C_{18}H_{15}O_7N_1$	356.07772	0.40	0.39	0.83	12	0.59
$C_{15}H_{19}O_9N_1$	356.09875	0.13	0.60	1.27	7	0.21
$C_{16}H_{23}O_8N_1$	356.13510	0.03	0.50	1.44	6	0.14
$C_{17}H_{10}O_9$	357.02521	0.01	0.53	0.59	13	0.68
$C_{16}H_{10}O_8N_2$	357.03649	0.14	0.50	0.63	13	0.80
$C_{18}H_{14}O_8$	357.06165	0.16	0.44	0.78	12	0.57
$C_{15}H_{18}O_{10}$	357.08272	0.00	0.67	1.20	7	0.20
$C_{12}H_{22}O_{10}S_1$	357.08607	−0.06	0.83	1.83	2	−0.67
$C_{14}H_{18}O_9N_2$	357.09397	0.04	0.64	1.29	7	0.20
$C_{16}H_{22}O_9$	357.11914	0.09	0.56	1.38	6	0.13
$C_{15}H_{22}O_8N_2$	357.13040	0.17	0.53	1.47	6	0.11
$C_{17}H_{26}O_8$	357.15552	0.08	0.47	1.53	5	0.08

Appendix A (*continued*)

Sum formula	Mass	Error (ppm)	O/C	H/C	DBE	AI_{mod}
$C_{18}H_{30}O_7$	357.19191	0.09	0.39	1.67	4	0.03
$C_{17}H_{13}O_8N_1$	358.05670	−0.39	0.47	0.76	12	0.63
$C_{14}H_{17}O_{10}N_1$	358.07796	−0.03	0.71	1.21	7	0.19
$C_{15}H_{21}O_9N_1$	358.11426	−0.26	0.60	1.40	6	0.11
$C_{16}H_{25}O_8N_1$	358.15073	−0.03	0.50	1.56	5	0.05
$C_{17}H_{12}O_9$	359.04094	0.23	0.53	0.71	12	0.60
$C_{14}H_{16}O_{11}$	359.06196	−0.07	0.79	1.14	7	0.18
$C_{18}H_{16}O_8$	359.07725	0.02	0.44	0.89	11	0.50
$C_{15}H_{20}O_8S_1$	359.08062	0.02	0.53	1.33	6	0.10
$C_{15}H_{20}O_{10}$	359.09838	0.03	0.67	1.33	6	0.10
$C_{12}H_{24}O_{10}S_1$	359.10180	0.16	0.83	2.00	1	−0.83
$C_{14}H_{20}O_9N_2$	359.10975	0.41	0.64	1.43	6	0.07
$C_{19}H_{20}O_7$	359.11353	−0.27	0.37	1.05	10	0.42
$C_{16}H_{24}O_9$	359.13480	0.12	0.56	1.50	5	0.04
$C_{15}H_{24}O_8N_2$	359.14598	−0.03	0.53	1.60	5	0.00
$C_{20}H_{24}O_6$	359.15003	0.05	0.30	1.20	9	0.35
$C_{17}H_{28}O_8$	359.17110	−0.12	0.47	1.65	4	0.00
$C_{17}H_{15}O_8N_1$	360.07258	0.25	0.47	0.88	11	0.54
$C_{14}H_{19}O_{10}N_1$	360.09370	0.22	0.71	1.36	6	0.06
$C_{18}H_{19}O_7N_1$	360.10884	−0.10	0.39	1.06	10	0.44
$C_{15}H_{23}O_9N_1$	360.13007	0.18	0.60	1.53	5	0.00
$C_{16}H_{10}O_{10}$	361.02003	−0.25	0.63	0.63	12	0.64
$C_{17}H_{14}O_9$	361.05650	−0.02	0.53	0.82	11	0.52
$C_{14}H_{18}O_9S_1$	361.05981	−0.18	0.64	1.29	6	0.06
$C_{14}H_{18}O_{11}$	361.07760	−0.10	0.79	1.29	6	0.06
$C_{11}H_{22}O_{11}S_1$	361.08109	0.23	1.00	2.00	1	−1.22
$C_{18}H_{18}O_8$	361.09292	0.08	0.44	1.00	10	0.43
$C_{15}H_{22}O_8S_1$	361.09623	−0.09	0.53	1.47	5	0.00
$C_{17}H_{18}O_7N_2$	361.10412	−0.01	0.41	1.06	10	0.48
$C_{12}H_{26}O_{10}S_1$	361.11740	0.02	0.83	2.17	0	−1.00
$C_{19}H_{22}O_7$	361.12929	0.04	0.37	1.16	9	0.35
$C_{16}H_{26}O_9$	361.15025	−0.43	0.56	1.63	4	−0.04
$C_{20}H_{26}O_6$	361.16563	−0.09	0.30	1.30	8	0.29
$C_{16}H_{13}O_9N_1$	362.05172	−0.10	0.56	0.81	11	0.57
$C_{17}H_{17}O_8N_1$	362.08809	−0.14	0.47	1.00	10	0.46
$C_{14}H_{21}O_{10}N_1$	362.10933	0.17	0.71	1.50	5	−0.06
$C_{18}H_{21}O_7N_1$	362.12455	0.07	0.39	1.17	9	0.37
$C_{19}H_{25}O_6N_1$	362.16097	0.16	0.32	1.32	8	0.30
$C_{16}H_{12}O_{10}$	363.03579	0.05	0.63	0.75	11	0.55
$C_{17}H_{16}O_9$	363.07219	0.09	0.53	0.94	10	0.44
$C_{14}H_{20}O_9S_1$	363.07551	−0.05	0.64	1.43	5	−0.06
$C_{16}H_{16}O_8N_2$	363.08332	−0.19	0.50	1.00	10	0.50
$C_{18}H_{20}O_8$	363.10855	0.02	0.44	1.11	9	0.36
$C_{17}H_{20}O_7N_2$	363.11971	−0.18	0.41	1.18	9	0.39
$C_{15}H_{24}O_{10}$	363.12976	0.25	0.67	1.60	4	−0.10
$C_{19}H_{24}O_7$	363.14493	0.01	0.37	1.26	8	0.29
$C_{18}H_{24}O_6N_2$	363.15606	−0.28	0.33	1.33	8	0.31
$C_{20}H_{28}O_6$	363.18132	0.02	0.30	1.40	7	0.24
$C_{16}H_{15}O_9N_1$	364.06752	0.32	0.56	0.94	10	0.48
$C_{17}H_{19}O_8N_1$	364.10382	0.08	0.47	1.12	9	0.38
$C_{18}H_{23}O_7N_1$	364.14012	−0.15	0.39	1.28	8	0.30
$C_{15}H_{10}O_{11}$	365.01512	0.23	0.73	0.67	11	0.58
$C_{16}H_{14}O_{10}$	365.05145	0.08	0.63	0.88	10	0.45
$C_{17}H_{18}O_9$	365.08784	0.09	0.53	1.06	9	0.36
$C_{14}H_{22}O_9S_1$	365.09133	0.42	0.64	1.57	4	−0.18
$C_{16}H_{18}O_8N_2$	365.09907	0.08	0.50	1.13	9	0.40
$C_{18}H_{22}O_8$	365.12420	0.02	0.44	1.22	8	0.29
$C_{17}H_{22}O_7N_2$	365.13542	−0.01	0.41	1.29	8	0.30
$C_{19}H_{26}O_7$	365.16062	0.12	0.37	1.37	7	0.23
$C_{16}H_{30}O_7S_1$	365.16396	0.03	0.44	1.88	2	−0.22
$C_{20}H_{30}O_6$	365.19693	−0.09	0.30	1.50	6	0.18
$C_{16}H_{17}O_9N_1$	366.08308	0.07	0.56	1.06	9	0.38

(*continued on next page*)

Appendix A (*continued*)

Sum formula	Mass	Error (ppm)	O/C	H/C	DBE	AI_{mod}
$C_{17}H_{21}O_8N_1$	366.11944	0.00	0.47	1.24	8	0.29
$C_{18}H_{25}O_7N_1$	366.15586	0.09	0.39	1.39	7	0.22
$C_{18}H_8O_9$	367.00956	0.01	0.50	0.44	15	0.78
$C_{15}H_{12}O_{11}$	367.03073	0.12	0.73	0.80	10	0.47
$C_{19}H_{12}O_8$	367.04587	−0.19	0.42	0.63	14	0.67
$C_{16}H_{16}O_8S_1$	367.04936	0.13	0.50	1.00	9	0.36
$C_{16}H_{16}O_{10}$	367.06709	0.05	0.63	1.00	9	0.36
$C_{15}H_{16}O_9N_2$	367.07829	−0.04	0.60	1.07	9	0.41
$C_{17}H_{20}O_9$	367.10345	−0.02	0.53	1.18	8	0.28
$C_{14}H_{24}O_9S_1$	367.10692	0.25	0.64	1.71	3	−0.29
$C_{16}H_{20}O_8N_2$	367.11467	−0.05	0.50	1.25	8	0.30
$C_{18}H_{24}O_8$	367.13983	−0.03	0.44	1.33	7	0.21
$C_{15}H_{28}O_8S_1$	367.14327	0.16	0.53	1.87	2	−0.30
$C_{17}H_{24}O_7N_2$	367.15107	−0.01	0.41	1.41	7	0.22
$C_{19}H_{28}O_5S_1$	367.15848	0.03	0.26	1.47	6	0.16
$C_{19}H_{28}O_7$	367.17626	0.09	0.37	1.47	6	0.16
$C_{16}H_{32}O_7S_1$	367.17958	−0.05	0.44	2.00	1	−0.30
$C_{20}H_{32}O_4S_1$	367.19480	−0.15	0.20	1.60	5	0.12
$C_{24}H_{48}O_2$	367.35823	0.20	0.08	2.00	1	0.00
$C_{15}H_{15}O_{10}N_1$	368.06238	0.16	0.67	1.00	9	0.39
$C_{16}H_{19}O_9N_1$	368.09873	0.07	0.56	1.19	8	0.29
$C_{17}H_{23}O_8N_1$	368.13513	0.11	0.47	1.35	7	0.21
$C_{18}H_{10}O_9$	369.02531	0.28	0.50	0.56	14	0.70
$C_{15}H_{14}O_{11}$	369.04618	−0.42	0.73	0.93	9	0.37
$C_{19}H_{14}O_8$	369.06169	0.27	0.42	0.74	13	0.60
$C_{16}H_{18}O_8S_1$	369.06497	0.02	0.50	1.13	8	0.27
$C_{18}H_{14}O_7N_2$	369.07284	0.04	0.39	0.78	13	0.68
$C_{16}H_{18}O_{10}$	369.08276	0.11	0.63	1.13	8	0.27
$C_{13}H_{22}O_{10}S_1$	369.08627	0.48	0.77	1.69	3	−0.43
$C_{15}H_{18}O_9N_2$	369.09397	0.04	0.60	1.20	8	0.29
$C_{17}H_{22}O_9$	369.11911	0.01	0.53	1.29	7	0.20
$C_{14}H_{26}O_9S_1$	369.12262	0.39	0.64	1.86	2	−0.41
$C_{16}H_{22}O_8N_2$	369.13024	−0.27	0.50	1.38	7	0.20
$C_{18}H_{26}O_8$	369.15550	0.02	0.44	1.44	6	0.14
$C_{19}H_{30}O_7$	369.19187	−0.02	0.37	1.58	5	0.10
$C_{16}H_{34}O_7S_1$	369.19520	−0.13	0.44	2.13	0	−0.39
$C_{15}H_{17}O_{10}N_1$	370.07795	−0.05	0.67	1.13	8	0.28
$C_{16}H_{21}O_9N_1$	370.11442	0.18	0.56	1.31	7	0.19
$C_{17}H_{25}O_8N_1$	370.15065	−0.24	0.47	1.47	6	0.13
$C_{18}H_{29}O_7N_1$	370.18713	0.01	0.39	1.61	5	0.07
$C_{17}H_8O_{10}$	371.00441	−0.16	0.59	0.47	14	0.75
$C_{18}H_{12}O_9$	371.04086	0.01	0.50	0.67	13	0.63
$C_{15}H_{16}O_9S_1$	371.04415	−0.21	0.60	1.07	8	0.26
$C_{15}H_{16}O_{11}$	371.06198	−0.01	0.73	1.07	8	0.26
$C_{14}H_{16}O_{10}N_2$	371.07338	0.43	0.71	1.14	8	0.29
$C_{19}H_{16}O_8$	371.07707	−0.46	0.42	0.84	12	0.53
$C_{16}H_{20}O_8S_1$	371.08067	0.16	0.50	1.25	7	0.18
$C_{16}H_{20}O_{10}$	371.09834	−0.08	0.63	1.25	7	0.18
$C_{15}H_{20}O_9N_2$	371.10958	−0.06	0.60	1.33	7	0.18
$C_{21}H_{24}O_2S_2$	371.11436	−0.36	0.10	1.14	10	0.39
$C_{17}H_{24}O_9$	371.13476	0.01	0.53	1.41	6	0.12
$C_{16}H_{24}O_8N_2$	371.14610	0.30	0.50	1.50	6	0.10
$C_{18}H_{28}O_8$	371.17117	0.08	0.44	1.56	5	0.07
$C_{17}H_{11}O_9N_1$	372.03618	0.20	0.53	0.65	13	0.70
$C_{15}H_{19}O_{10}N_1$	372.09363	0.03	0.67	1.27	7	0.17
$C_{19}H_{19}O_7N_1$	372.10895	0.20	0.37	1.00	11	0.48
$C_{16}H_{23}O_9N_1$	372.13008	0.20	0.56	1.44	6	0.10
$C_{17}H_{27}O_8N_1$	372.16648	0.24	0.47	1.59	5	0.04
$C_{17}H_{10}O_{10}$	373.02013	0.03	0.59	0.59	13	0.67
$C_{18}H_{14}O_9$	373.05648	−0.07	0.50	0.78	12	0.56
$C_{15}H_{18}O_9S_1$	373.05997	0.25	0.60	1.20	7	0.16
$C_{17}H_{14}O_8N_2$	373.06766	−0.21	0.47	0.82	12	0.64

Appendix A (*continued*)

Sum formula	Mass	Error (ppm)	O/C	H/C	DBE	AI_{mod}
$C_{15}H_{18}O_{11}$	373.07764	0.01	0.73	1.20	7	0.16
$C_{19}H_{18}O_{8}$	373.09295	0.16	0.42	0.95	11	0.47
$C_{16}H_{22}O_{8}S_{1}$	373.09617	−0.25	0.50	1.38	6	0.09
$C_{16}H_{22}O_{10}$	373.11402	0.00	0.63	1.38	6	0.09
$C_{15}H_{22}O_{9}N_{2}$	373.12532	0.18	0.60	1.47	6	0.06
$C_{20}H_{22}O_{7}$	373.12927	−0.02	0.35	1.10	10	0.39
$C_{17}H_{26}O_{9}$	373.15034	−0.18	0.53	1.53	5	0.04
$C_{16}H_{26}O_{8}N_{2}$	373.16154	−0.27	0.50	1.63	5	0.00
$C_{21}H_{26}O_{6}$	373.16552	−0.38	0.29	1.24	9	0.33
$C_{18}H_{30}O_{8}$	373.18680	0.02	0.44	1.67	4	0.00
$C_{17}H_{13}O_{9}N_{1}$	374.05171	−0.12	0.53	0.76	12	0.61
$C_{14}H_{17}O_{11}N_{1}$	374.07290	0.04	0.79	1.21	7	0.13
$C_{18}H_{17}O_{8}N_{1}$	374.08826	0.32	0.44	0.94	11	0.50
$C_{15}H_{21}O_{10}N_{1}$	374.10933	0.16	0.67	1.40	6	0.06
$C_{16}H_{25}O_{9}N_{1}$	374.14568	0.07	0.56	1.56	5	0.00
$C_{17}H_{12}O_{10}$	375.03576	−0.03	0.59	0.71	12	0.58
$C_{14}H_{16}O_{12}$	375.05679	−0.29	0.86	1.14	7	0.13
$C_{18}H_{16}O_{9}$	375.07216	0.01	0.50	0.89	11	0.48
$C_{15}H_{20}O_{9}S_{1}$	375.07560	0.20	0.60	1.33	6	0.05
$C_{15}H_{20}O_{11}$	375.09337	0.23	0.73	1.33	6	0.05
$C_{19}H_{20}O_{8}$	375.10856	0.05	0.42	1.05	10	0.40
$C_{16}H_{24}O_{8}S_{1}$	375.11181	−0.27	0.50	1.50	5	0.00
$C_{16}H_{24}O_{10}$	375.12963	−0.11	0.63	1.50	5	0.00
$C_{13}H_{28}O_{10}S_{1}$	375.13319	0.39	0.77	2.15	0	−0.86
$C_{27}H_{20}O_{2}$	375.13921	0.42	0.07	0.74	18	0.65
$C_{20}H_{24}O_{7}$	375.14499	0.17	0.35	1.20	9	0.33
$C_{17}H_{28}O_{9}$	375.16601	−0.12	0.53	1.65	4	−0.04
$C_{21}H_{28}O_{6}$	375.18118	−0.35	0.29	1.33	8	0.28
$C_{16}H_{11}O_{10}N_{1}$	376.03088	−0.37	0.63	0.69	12	0.65
$C_{17}H_{15}O_{9}N_{1}$	376.06743	0.07	0.53	0.88	11	0.52
$C_{18}H_{19}O_{8}N_{1}$	376.10380	0.03	0.44	1.06	10	0.42
$C_{15}H_{23}O_{10}N_{1}$	376.12490	−0.05	0.67	1.53	5	−0.06
$C_{19}H_{23}O_{7}N_{1}$	376.14017	−0.02	0.37	1.21	9	0.34
$C_{16}H_{27}O_{9}N_{1}$	376.16120	−0.28	0.56	1.69	4	−0.10
$C_{16}H_{10}O_{11}$	377.01512	0.23	0.69	0.63	12	0.62
$C_{10}H_{18}O_{11}S_{2}$	377.02168	−0.26	1.10	1.80	2	−2.20
$C_{12}H_{14}O_{12}N_{2}$	377.04745	0.14	1.00	1.17	7	0.00
$C_{17}H_{14}O_{10}$	377.05148	0.16	0.59	0.82	11	0.50
$C_{16}H_{14}O_{9}N_{2}$	377.06270	0.12	0.56	0.88	11	0.58
$C_{18}H_{18}O_{9}$	377.08787	0.17	0.50	1.00	10	0.41
$C_{15}H_{22}O_{9}S_{1}$	377.09133	0.41	0.60	1.47	5	−0.05
$C_{17}H_{18}O_{8}N_{2}$	377.09898	−0.16	0.47	1.06	10	0.45
$C_{15}H_{22}O_{11}$	377.10893	−0.01	0.73	1.47	5	−0.05
$C_{12}H_{26}O_{11}S_{1}$	377.11224	−0.17	0.92	2.17	0	−1.18
$C_{19}H_{22}O_{8}$	377.12420	0.02	0.42	1.16	9	0.33
$C_{18}H_{22}O_{7}N_{2}$	377.13545	0.07	0.39	1.22	9	0.36
$C_{20}H_{26}O_{7}$	377.16060	0.06	0.35	1.30	8	0.27
$C_{21}H_{30}O_{6}$	377.19688	−0.22	0.29	1.43	7	0.22
$C_{16}H_{13}O_{10}N_{1}$	378.04674	0.19	0.63	0.81	11	0.55
$C_{17}H_{17}O_{9}N_{1}$	378.08309	0.09	0.53	1.00	10	0.43
$C_{18}H_{21}O_{8}N_{1}$	378.11947	0.08	0.44	1.17	9	0.35
$C_{16}H_{12}O_{11}$	379.03061	−0.20	0.69	0.75	11	0.52
$C_{17}H_{16}O_{10}$	379.06705	−0.05	0.59	0.94	10	0.42
$C_{16}H_{16}O_{9}N_{2}$	379.07829	−0.04	0.56	1.00	10	0.47
$C_{18}H_{20}O_{9}$	379.10346	0.01	0.50	1.11	9	0.33
$C_{17}H_{20}O_{8}N_{2}$	379.11466	−0.08	0.47	1.18	9	0.36
$C_{19}H_{24}O_{8}$	379.13982	−0.06	0.42	1.26	8	0.27
$C_{18}H_{24}O_{7}N_{2}$	379.15098	−0.25	0.39	1.33	8	0.28
$C_{20}H_{28}O_{7}$	379.17620	−0.07	0.35	1.40	7	0.21
$C_{16}H_{15}O_{10}N_{1}$	380.06232	0.00	0.63	0.94	10	0.45
$C_{17}H_{19}O_{9}N_{1}$	380.09873	0.07	0.53	1.12	9	0.35
$C_{18}H_{23}O_{8}N_{1}$	380.13508	−0.03	0.44	1.28	8	0.27

(*continued on next page*)

Appendix A (*continued*)

Sum formula	Mass	Error (ppm)	O/C	H/C	DBE	AI_{mod}
$C_{19}H_{27}O_7N_1$	380.17155	0.19	0.37	1.42	7	0.21
$C_{16}H_{14}O_{11}$	381.04630	−0.09	0.69	0.88	10	0.43
$C_{17}H_{18}O_{10}$	381.08270	−0.05	0.59	1.06	9	0.33
$C_{16}H_{18}O_9N_2$	381.09396	0.02	0.56	1.13	9	0.37
$C_{18}H_{22}O_9$	381.11907	−0.09	0.50	1.22	8	0.26
$C_{17}H_{22}O_8N_2$	381.13030	−0.10	0.47	1.29	8	0.27
$C_{19}H_{26}O_8$	381.15545	−0.11	0.42	1.37	7	0.20
$C_{20}H_{30}O_5S_1$	381.17403	−0.23	0.25	1.50	6	0.15
$C_{20}H_{30}O_7$	381.19190	0.06	0.35	1.50	6	0.15
$C_{16}H_{17}O_{10}N_1$	382.07804	0.18	0.63	1.06	9	0.35
$C_{17}H_{21}O_9N_1$	382.11437	0.04	0.53	1.24	8	0.26
$C_{18}H_{25}O_8N_1$	382.15069	−0.13	0.44	1.39	7	0.19
$C_{19}H_{29}O_7N_1$	382.18702	−0.28	0.37	1.53	6	0.14
$C_{19}H_{12}O_9$	383.04075	−0.28	0.47	0.63	14	0.66
$C_{16}H_{16}O_{11}$	383.06198	−0.01	0.69	1.00	9	0.33
$C_{15}H_{16}O_{10}N_2$	383.07309	−0.33	0.67	1.07	9	0.38
$C_{17}H_{20}O_{10}$	383.09836	−0.03	0.59	1.18	8	0.25
$C_{14}H_{24}O_{10}S_1$	383.10182	0.20	0.71	1.71	3	−0.38
$C_{16}H_{20}O_9N_2$	383.10964	0.09	0.56	1.25	8	0.26
$C_{18}H_{24}O_9$	383.13471	−0.12	0.50	1.33	7	0.19
$C_{17}H_{24}O_8N_2$	383.14588	−0.28	0.47	1.41	7	0.18
$C_{19}H_{28}O_8$	383.17112	−0.06	0.42	1.47	6	0.13
$C_{20}H_{32}O_5S_1$	383.18973	−0.10	0.25	1.60	5	0.09
$C_{20}H_{32}O_7$	383.20761	0.22	0.35	1.60	5	0.09
$C_{18}H_{11}O_9N_1$	384.03605	−0.14	0.50	0.61	14	0.72
$C_{15}H_{15}O_{11}N_1$	384.05721	−0.06	0.73	1.00	9	0.35
$C_{16}H_{19}O_{10}N_1$	384.09367	0.13	0.63	1.19	8	0.25
$C_{17}H_{23}O_9N_1$	384.12998	−0.06	0.53	1.35	7	0.17
$C_{18}H_{27}O_8N_1$	384.16650	0.28	0.44	1.50	6	0.12
$C_{18}H_{10}O_{10}$	385.02009	−0.08	0.56	0.56	14	0.69
$C_{15}H_{14}O_{12}$	385.04130	0.13	0.80	0.93	9	0.33
$C_{19}H_{14}O_9$	385.05651	0.01	0.47	0.74	13	0.59
$C_{16}H_{18}O_{11}$	385.07760	−0.09	0.69	1.13	8	0.24
$C_{15}H_{18}O_{10}N_2$	385.08881	−0.15	0.67	1.20	8	0.25
$C_{17}H_{22}O_8S_1$	385.09632	0.15	0.47	1.29	7	0.17
$C_{17}H_{22}O_{10}$	385.11400	−0.05	0.59	1.29	7	0.17
$C_{16}H_{22}O_9N_2$	385.12538	0.33	0.56	1.38	7	0.16
$C_{18}H_{26}O_9$	385.15037	−0.09	0.50	1.44	6	0.11
$C_{19}H_{30}O_8$	385.18674	−0.13	0.42	1.58	5	0.07
$C_{16}H_{34}O_8S_1$	385.19002	−0.37	0.50	2.13	0	−0.45
$C_{20}H_{34}O_7$	385.22331	0.34	0.35	1.70	4	0.03
$C_{15}H_{17}O_{11}N_1$	386.07293	0.12	0.73	1.13	8	0.24
$C_{16}H_{21}O_{10}N_1$	386.10924	−0.08	0.63	1.31	7	0.15
$C_{17}H_{25}O_9N_1$	386.14560	−0.14	0.53	1.47	6	0.09
$C_{18}H_{29}O_8N_1$	386.18217	0.33	0.44	1.61	5	0.04
$C_{18}H_{12}O_{10}$	387.03571	−0.16	0.56	0.67	13	0.62
$C_{15}H_{16}O_{12}$	387.05688	−0.05	0.80	1.07	8	0.22
$C_{19}H_{16}O_9$	387.07228	0.32	0.47	0.84	12	0.52
$C_{16}H_{20}O_9S_1$	387.07553	0.01	0.56	1.25	7	0.14
$C_{16}H_{20}O_{11}$	387.09325	−0.09	0.69	1.25	7	0.14
$C_{15}H_{20}O_{10}N_2$	387.10463	0.29	0.67	1.33	7	0.13
$C_{20}H_{20}O_8$	387.10850	−0.11	0.40	1.00	11	0.44
$C_{17}H_{24}O_{10}$	387.12963	−0.10	0.59	1.41	6	0.08
$C_{21}H_{24}O_7$	387.14490	−0.07	0.33	1.14	10	0.37
$C_{18}H_{28}O_9$	387.16606	0.01	0.50	1.56	5	0.04
$C_{18}H_{15}O_9N_1$	388.06729	−0.30	0.50	0.83	12	0.56
$C_{15}H_{19}O_{11}N_1$	388.08861	0.20	0.73	1.27	7	0.12
$C_{19}H_{19}O_8N_1$	388.10370	−0.23	0.42	1.00	11	0.46
$C_{16}H_{23}O_{10}N_1$	388.12498	0.16	0.63	1.44	6	0.05
$C_{20}H_{23}O_7N_1$	388.14010	−0.19	0.35	1.15	10	0.39
$C_{17}H_{27}O_9N_1$	388.16138	0.19	0.53	1.59	5	0.00
$C_{18}H_{14}O_6S_2$	389.01573	−0.44	0.33	0.78	12	0.54

Appendix A (*continued*)

Sum formula	Mass	Error (ppm)	O/C	H/C	DBE	AI_{mod}
$C_{18}H_{14}O_{10}$	389.05144	0.05	0.56	0.78	12	0.54
$C_{15}H_{18}O_{10}S_1$	389.05483	0.10	0.67	1.20	7	0.11
$C_{17}H_{14}O_9N_2$	389.06251	−0.37	0.53	0.82	12	0.62
$C_{15}H_{18}O_{12}$	389.07246	−0.23	0.80	1.20	7	0.11
$C_{26}H_{14}O_4$	389.08190	−0.08	0.15	0.54	20	0.75
$C_{19}H_{18}O_9$	389.08776	−0.12	0.47	0.95	11	0.45
$C_{16}H_{22}O_9S_1$	389.09108	−0.25	0.56	1.38	6	0.05
$C_{16}H_{22}O_{11}$	389.10891	−0.06	0.69	1.38	6	0.05
$C_{13}H_{26}O_{11}S_1$	389.11236	0.14	0.85	2.00	1	−0.85
$C_{20}H_{22}O_8$	389.12417	−0.05	0.40	1.10	10	0.38
$C_{17}H_{26}O_{10}$	389.14528	−0.10	0.59	1.53	5	0.00
$C_{14}H_{30}O_{10}S_1$	389.14874	0.12	0.71	2.14	0	−0.75
$C_{21}H_{26}O_7$	389.16064	0.16	0.33	1.24	9	0.31
$C_{18}H_{30}O_9$	389.18179	0.21	0.50	1.67	4	−0.04
$C_{22}H_{30}O_6$	389.19696	−0.01	0.27	1.36	8	0.26
$C_{17}H_{13}O_{10}N_1$	390.04649	−0.46	0.59	0.76	12	0.59
$C_{18}H_{17}O_9N_1$	390.08307	0.04	0.50	0.94	11	0.48
$C_{15}H_{21}O_{11}N_1$	390.10417	−0.04	0.73	1.40	6	0.00
$C_{19}H_{21}O_8N_1$	390.11944	0.00	0.42	1.11	10	0.39
$C_{16}H_{25}O_{10}N_1$	390.14056	−0.02	0.63	1.56	5	−0.05
$C_{20}H_{25}O_7N_1$	390.15595	0.32	0.35	1.25	9	0.32
$C_{17}H_{12}O_{11}$	391.03074	0.14	0.65	0.71	12	0.57
$C_{18}H_{16}O_{10}$	391.06707	0.00	0.56	0.89	11	0.46
$C_{15}H_{20}O_{10}S_1$	391.07063	0.48	0.67	1.33	6	0.00
$C_{17}H_{16}O_9N_2$	391.07824	−0.16	0.53	0.94	11	0.52
$C_{15}H_{20}O_{12}$	391.08829	0.23	0.80	1.33	6	0.00
$C_{26}H_{16}O_4$	391.09777	0.48	0.15	0.62	19	0.71
$C_{19}H_{20}O_9$	391.10343	−0.07	0.47	1.05	10	0.38
$C_{18}H_{20}O_8N_2$	391.11455	−0.36	0.44	1.11	10	0.42
$C_{16}H_{24}O_{11}$	391.12459	0.01	0.69	1.50	5	−0.05
$C_{13}H_{28}O_{11}S_1$	391.12796	0.01	0.85	2.15	0	−1.00
$C_{27}H_{20}O_3$	391.13386	−0.28	0.11	0.74	18	0.65
$C_{20}H_{24}O_8$	391.13987	0.07	0.40	1.20	9	0.31
$C_{19}H_{24}O_7N_2$	391.15097	−0.27	0.37	1.26	9	0.33
$C_{17}H_{28}O_{10}$	391.16098	0.02	0.59	1.65	4	−0.08
$C_{21}H_{28}O_7$	391.17621	−0.04	0.33	1.33	8	0.26
$C_{22}H_{32}O_6$	391.21265	0.10	0.27	1.45	7	0.21
$C_{17}H_{15}O_{10}N_1$	392.06233	0.03	0.59	0.88	11	0.50
$C_{18}H_{19}O_9N_1$	392.09880	0.24	0.50	1.06	10	0.40
$C_{19}H_{23}O_8N_1$	392.13506	−0.08	0.42	1.21	9	0.32
$C_{20}H_{27}O_7N_1$	392.17148	0.01	0.35	1.35	8	0.26
$C_{17}H_{14}O_{11}$	393.04641	0.19	0.65	0.82	11	0.48
$C_{18}H_{18}O_{10}$	393.08276	0.10	0.56	1.00	10	0.38
$C_{17}H_{18}O_9N_2$	393.09394	−0.04	0.53	1.06	10	0.43
$C_{12}H_{26}O_{12}S_1$	393.10709	−0.33	1.00	2.17	0	−1.40
$C_{19}H_{22}O_9$	393.11908	−0.07	0.47	1.16	9	0.31
$C_{18}H_{22}O_8N_2$	393.13024	−0.25	0.44	1.22	9	0.33
$C_{20}H_{26}O_8$	393.15546	−0.08	0.40	1.30	8	0.25
$C_{21}H_{30}O_7$	393.19191	0.08	0.33	1.43	7	0.20
$C_{17}H_{17}O_{10}N_1$	394.07793	−0.10	0.59	1.00	10	0.41
$C_{18}H_{21}O_9N_1$	394.11431	−0.11	0.50	1.17	9	0.32
$C_{19}H_{25}O_8N_1$	394.15076	0.05	0.42	1.32	8	0.25
$C_{20}H_{29}O_7N_1$	394.18715	0.06	0.35	1.45	7	0.19
$C_{16}H_{12}O_{12}$	395.02565	0.13	0.75	0.75	11	0.50
$C_{20}H_{12}O_9$	395.04087	0.04	0.45	0.60	15	0.68
$C_{17}H_{16}O_{11}$	395.06189	−0.24	0.65	0.94	10	0.39
$C_{16}H_{16}O_{10}N_2$	395.07319	−0.07	0.63	1.00	10	0.44
$C_{18}H_{20}O_{10}$	395.09838	0.02	0.56	1.11	9	0.31
$C_{17}H_{20}O_9N_2$	395.10956	−0.11	0.53	1.18	9	0.33
$C_{19}H_{24}O_9$	395.13474	−0.04	0.47	1.26	8	0.24
$C_{18}H_{24}O_8N_2$	395.14592	−0.18	0.44	1.33	8	0.25
$C_{20}H_{28}O_6S_1$	395.15333	−0.13	0.30	1.40	7	0.19

(*continued on next page*)

Appendix A (*continued*)

Sum formula	Mass	Error (ppm)	O/C	H/C	DBE	AI_{mod}
$C_{20}H_{28}O_8$	395.17114	0.00	0.40	1.40	7	0.19
$C_{21}H_{32}O_7$	395.20743	−0.25	0.33	1.52	6	0.14
$C_{16}H_{15}O_{11}N_1$	396.05718	−0.14	0.69	0.94	10	0.42
$C_{17}H_{19}O_{10}N_1$	396.09354	−0.20	0.59	1.12	9	0.32
$C_{18}H_{23}O_9N_1$	396.12995	−0.14	0.50	1.28	8	0.24
$C_{19}H_{27}O_8N_1$	396.16632	−0.18	0.42	1.42	7	0.18
$C_{19}H_{10}O_{10}$	397.02004	−0.20	0.53	0.53	15	0.71
$C_{16}H_{14}O_{12}$	397.04115	−0.25	0.75	0.88	10	0.40
$C_{20}H_{14}O_9$	397.05636	−0.37	0.45	0.70	14	0.61
$C_{17}H_{18}O_9S_1$	397.06002	0.36	0.53	1.06	9	0.30
$C_{17}H_{18}O_{11}$	397.07759	−0.11	0.65	1.06	9	0.30
$C_{16}H_{18}O_{10}N_2$	397.08887	0.00	0.63	1.13	9	0.33
$C_{18}H_{22}O_{10}$	397.11400	−0.05	0.56	1.22	8	0.23
$C_{17}H_{22}O_9N_2$	397.12518	−0.19	0.53	1.29	8	0.24
$C_{19}H_{26}O_9$	397.15034	−0.17	0.47	1.37	7	0.17
$C_{20}H_{30}O_8$	397.18674	−0.13	0.40	1.50	6	0.13
$C_{18}H_{38}O_7S_1$	397.22658	0.08	0.39	2.11	0	−0.33
$C_{17}H_5O_{11}N_1$	397.97910	0.29	0.65	0.29	16	0.95
$C_{16}H_{17}O_{11}N_1$	398.07294	0.14	0.69	1.06	9	0.32
$C_{17}H_{21}O_{10}N_1$	398.10925	−0.05	0.59	1.24	8	0.23
$C_{18}H_{25}O_9N_1$	398.14555	−0.26	0.50	1.39	7	0.16
$C_{19}H_{29}O_8N_1$	398.18205	0.02	0.42	1.53	6	0.11
$C_{19}H_{12}O_{10}$	399.03582	0.12	0.53	0.63	14	0.64
$C_{16}H_{16}O_{12}$	399.05686	−0.10	0.75	1.00	9	0.30
$C_{20}H_{16}O_9$	399.07221	0.14	0.45	0.80	13	0.55
$C_{17}H_{20}O_9S_1$	399.07535	−0.44	0.53	1.18	8	0.22
$C_{17}H_{20}O_{11}$	399.09327	−0.04	0.65	1.18	8	0.22
$C_{16}H_{20}O_{10}N_2$	399.10453	0.03	0.63	1.25	8	0.22
$C_{18}H_{24}O_8S_1$	399.11181	−0.26	0.44	1.33	7	0.15
$C_{18}H_{24}O_{10}$	399.12959	−0.20	0.56	1.33	7	0.15
$C_{17}H_{24}O_9N_2$	399.14082	−0.21	0.53	1.41	7	0.14
$C_{19}H_{28}O_9$	399.16601	−0.12	0.47	1.47	6	0.10
$C_{20}H_{32}O_8$	399.20242	−0.05	0.40	1.60	5	0.06

REFERENCES

Alvarez-Salgado X. A., Figueiras F. G., Perez F. F., Groom S., Nogueira E., Borges A., Chou L., Castro C. G., Moncoiffe G., Rios A. F., Miller A. E. J., Frankignoulle M., Savidge G. and Wollast R. (2003) The Portugal coastal counter current off NW Spain: new insights on its biogeochemical variability. *Prog. Oceanogr.* **56**, 281–321.

Amon R. M. W. and Benner R. (1996) Bacterial utilization of different size classes of dissolved organic matter. *Limnol. Oceanogr.* **41**, 41–51.

Bauer J. E., Reimers C. E., Druffel E. R. M. and Williams P. M. (1995) Isotopic constraints on carbon exchange between deep ocean sediments and sea water. *Nature* **373**, 686–689.

Berner R. A. (1982) Burial of organic carbon and pyrite sulfur in the modern ocean; its geochemical and environmental significance. *Am. J. Sci.* **282**, 451.

Birgel D., Stein R. and Hefter J. (2004) Aliphatic lipids in recent sediments of the Fram Strait/Yermak Plateau (Arctic Ocean): composition, sources and transport processes. *Mar. Chem.* **88**, 127–160.

Burdige D. J., Berelson W. M., Coale K. H., McManus J. and Johnson K. S. (1999) Fluxes of dissolved organic carbon from California continental margin sediments. *Geochim. Cosmochim. Acta* **63**, 1507–1515.

Burdige D. J., Dennis A. H. and Craig A. C. (2002) Sediment Pore Waters, Biogeochemistry of Marine Dissolved Organic Matter. Academic Press, San Diego.

Burdige D. J. and Gardner K. G. (1998) Molecular weight distribution of dissolved organic carbon in marine sediment pore waters. *Mar. Chem.* **62**, 45–64.

Burdige D. J. and Zheng S. (1998) The biogeochemical cycling of dissolved organic nitrogen in estuarine sediments. *Limnol. Oceanogr.* **43**, 1796–1813.

Canuel E. A. and Martens C. S. (1996) Reactivity of recently deposited organic matter: degradation of lipid compounds near the sediment–water interface. *Geochim. Cosmochim. Acta* **60**, 1793–1806.

Coelho H. S., Neves R. J. J., White M., Leitao P. C. and Santos A. J. (2002) A model for ocean circulation on the Iberian coast. *J. Mar. Sys.* **32**, 153–179.

Decesari S., Facchini M. C., Matta E., Mircea M., Fuzzi S., Chughtai A. R. and Smith D. M. (2002) Water soluble organic compounds formed by oxidation of soot. *Atmos. Environ* **36**, 1827–1832.

Dias J. M. A., Jouanneau J. M., Gonzalez R., Araujo M. F., Drago T., Garcia C., Oliveira A., Rodrigues A., Vitorino J. and Weber O. (2002) Present day sedimentary processes on the northern Iberian shelf. *Prog. Oceanogr.* **52**, 249–259.

Dittmar T. and Koch B. P. (2006) Thermogenic organic matter dissolved in the abyssal ocean. *Mar. Chem.* **102**, 208–217.

Dittmar T., Koch B., Hertkorn N. and Kattner G. (2008) A simple and efficient method for the solid-phase extraction of dissolved organic matter (SPE-DOM) from seawater. *Limnol. Oceanogr. Methods* **6**, 230–235.

Eglinton G. and Hamilton R. J. (1967) Leaf epicular waxes. *Science*, 208.

Einsiedl F., Hertkorn N., Wolf M., Frommberger M., Schmitt-Kopplin P. and Koch B. P. (2007) Rapid biotic molecular transformation of fulvic acids in a karst aquifer. *Geochim. Cosmochim. Acta* **71**, 5474–5482.

Ertel J. R. and Hedges J. I. (1984) The lignin component of humic substances: distribution among soil and sedimentary humic, fulvic, and base-insoluble fractions. *Geochim. Cosmochim. Acta* **48**, 2065–2074.

Ertel J. R. and Hedges J. I. (1985) Sources of sedimentary humic substances: vascular plant debris. *Geochim. Cosmochim. Acta* **49**, 2097–2107.

Frouin R., Fiúza A. F. G., Ambar I. and Boyd T. J. (1990) Observations of a poleward surface current off the coasts of Portugal and Spain during winter. *J. Geophys. Res.* **95**, 679–691.

Goñi M. A. and Hedges J. I. (1995) Sources and reactivities of marine-derived organic matter in coastal sediments as determined by alkaline CuO oxidation. *Geochim. Cosmochim. Acta* **59**, 2965–2981.

Goñi M. A., Nelson B., Blanchette R. A. and Hedges J. I. (1993) Fungal degradation of wood lignins: geochemical perspectives from CuO-derived phenolic dimers and monomers. *Geochim. Cosmochim. Acta* **57**, 3985–4002.

Goñi M. A., Yunker M. B., Macdonald R. W. and Eglinton T. I. (2000) Distribution and sources of organic biomarkers in arctic sediments from the Mackenzie River and Beaufort Shelf. *Mar. Chem.* **71**, 23–51.

Hedges J. I., Blanchette R. A., Weliky K. and Devol A. H. (1988) Effects of fungal degradation on the CuO oxidation products of lignin: a controlled laboratory study. *Geochim. Cosmochim. Acta* **52**, 2717–2726.

Hedges J. I., Clark W. A., Quay P. D., Richey J. E. and Devol A. H. (1986) Compositions and fluxes of particulate organic material in the Amazon River. *Limnol. Oceanogr.* **31**, 717–738.

Hedges J. I., Eglinton G., Hatcher P. G., Kirchman D. L., Arnosti C., Derenne S., Evershed R. P., Kögel-Knabner I., de Leeuw J. W. and Littke R. (2000) The molecularly-uncharacterized component of nonliving organic matter in natural environments. *Org. Geochem.* **31**, 945–958.

Hedges J. I. and Ertel J. R. (1982) Characterization of lignin by gas capillary chromatography of cupric oxide oxidation products. *Anal. Chem.* **54**, 174–178.

Hedges J. I., Hatcher P. G., Ertel J. R. and Meyers-Schulte K. J. (1992) A comparison of dissolved humic substances from seawater with Amazon River counterparts by ^{13}C-NMR spectrometry. *Geochim. Cosmochim. Acta* **56**, 1753–1757.

Hedges J. I. and Keil R. G. (1995) Sedimentary organic matter preservation: an assessment and speculative synthesis. *Mar. Chem.* **49**, 81–115.

Henrichs S. M. (1992) Early diagenesis of organic matter in marine sediments: progress and perplexity. *Mar. Chem.* **39**, 119–149.

Hertkorn N., Benner R., Frommberger M., Schmitt-Kopplin P., Witt M., Kaiser K., Kettrup A. and Hedges J. I. (2006) Characterization of a major refractory component of marine dissolved organic matter. *Geochim. Cosmochim. Acta* **70**, 2990–3010.

Hinrichs K.-U., Summons R. E., Orphan V., Sylva S. P. and Hayes J. M. (2000) Molecular and isotopic analyses of anaerobic methane-oxidizing communities in marine sediments. *Org. Geochem.* **31**, 1685–1701.

Hockaday W. C., Grannas A. M., Kim S. and Hatcher P. G. (2006) Direct molecular evidence for the degradation and mobility of black carbon in soils from ultrahigh-resolution mass spectral analysis of dissolved organic matter from a fire-impacted forest soil. *Org. Geochem.* **37**, 501–510.

Hopkinson C. S., Buffam I., Hobbie J., Vallino J., Perdue M., Eversmeyer B., Prahl F., Covert J., Hodson R. and Moran M. A. (1998) Terrestrial inputs of organic matter to coastal ecosystems: an intercomparison of chemical characteristics and bioavailability. *Biogeochemistry* **43**, 211–234.

Janssen F., Huettel M. and Witte U. (2005) Pore-water advection and solute fluxes in permeable marine sediments(II): benthic respiration at three sandy sites with different permeabilities (German Bight, North Sea). *Limnol. Oceanogr.* **50**, 779–792.

Jouanneau J. M., Weber O., Drago T., Rodrigues A., Oliveira A., Dias J. M. A., Garcia C., Schmidt S. and Reyss J. L. (2002) Recent sedimentation and sedimentary budgets on the western Iberian shelf. *Prog. Oceanogr.* **52**, 261–275.

Kim S., Kaplan L. A., Benner R. and Hatcher P. G. (2004) Hydrogen-deficient molecules in natural riverine water samples – evidence for the existence of black carbon in DOM. *Mar. Chem.* **92**, 225–234.

Kim S., Kaplan L. A. and Hatcher P. G. (2006) Biodegradable dissolved organic matter in a temperate and a tropical stream determined from ultra-high resolution mass spectrometry. *Limnol. Oceanogr.* **51**, 1054–1063.

Kim S., Kramer R. W. and Hatcher P. G. (2003) Graphical method for analysis of ultrahigh-resolution broadband mass spectra of natural organic matter, the van Krevelen diagram. *Anal. Chem.* **75**, 5336–5344.

Koch B. P. and Dittmar T. (2006) From mass to structure: an aromaticity index for high-resolution mass data of natural organic matter. *Rapid Commun. Mass Spectrom.* **20**, 926.

Koch B. P., Dittmar T., Witt M. and Kattner G. (2007) Fundamentals of molecular formula assignment to ultrahigh resolution mass data of natural organic matter. *Anal. Chem.* **79**, 1758–1763.

Koch B. P., Ludwichowski K. U., Kattner G., Dittmar T. and Witt M. (2008) Advanced characterization of marine dissolved organic matter by combining reversed-phase liquid chromatography and FT-ICR-MS. *Mar. Chem.* **111**, 233–241.

Koch B. P., Witt M., Engbrodt R., Dittmar T. and Kattner G. (2005) Molecular formulae of marine and terrigenous dissolved organic matter detected by electrospray ionization Fourier transform ion cyclotron resonance mass spectrometry. *Geochim. Cosmochim. Acta* **69**, 3299–3308.

Kramer R. W., Kujawinski E. B. and Hatcher P. G. (2004) Identification of black carbon derived structures in a volcanic ash soil humic acid by fourier transform ion cyclotron resonance mass spectrometry. *Environ. Sci. Technol.* **38**, 3387–3395.

Kujawinski E. B., Del Vecchio R., Blough N. V., Klein G. C. and Marshall A. G. (2004) Probing molecular-level transformations of dissolved organic matter: insights on photochemical degradation and protozoan modification of DOM from electrospray ionization Fourier transform ion cyclotron resonance mass spectrometry. *Mar. Chem.* **92**, 23–37.

Kujawinski E. B., Freitas M. A., Zang X., Hatcher P. G., Green-Church K. B. and Jones R. B. (2002a) The application of electrospray ionization mass spectrometry (ESI MS) to the structural characterization of natural organic matter. *Org. Geochem.* **33**, 171–180.

Kujawinski E. B., Hatcher P. G. and Freitas M. A. (2002b) High-resolution Fourier transform ion cyclotron resonance mass spectrometry of humic and fulvic acids: improvements and comparisons. *Anal. Chem.* **74**, 413–419.

Lam B., Baer A., Alaee M., Lefebvre B., Moser A. and Williams A., et al. (2007) Major Structural Components in Freshwater Dissolved Organic Matter. *Environ. Sci. Technol.* **41**, 8240–8247.

Ludwig W., Probst J. L. and Kempe S. (1996) Predicting the oceanic input of organic carbon by continental erosion. *Global Biogeochem. Cycles* **10**, 23–41.

McCallister S. L., Bauer J. E., Ducklow H. W. and Canuel E. A. (2006) Sources of estuarine dissolved and particulate organic matter: a multi-tracer approach. *Org. Geochem.* **37**, 454–468.

Mead R. N. and Goñi M. A. (2008) Matrix protected organic matter in a river dominated margin: a possible mechanism to sequester terrestrial organic matter? *Geochim. Cosmochim. Acta* **72**, 2673–2686.

Medeiros P. M. and Simoneit B. R. T. (2008) Multi-biomarker characterization of sedimentary organic carbon in small rivers draining the Northwestern United States. *Org. Geochem.* **39**, 52–74.

Oliveira A., Rocha F., Rodrigues A., Jouanneau J., Dias A., Weber O. and Gomes C. (2002) Clay minerals from the sedimentary cover from the Northwest Iberian shelf. *Prog. Oceanogr.* **52**, 233–247.

Opsahl S. and Benner R. (1995) Early diagenesis of vascular plant tissues: lignin and cutin decomposition and biogeochemical implications. *Geochim. Cosmochim. Acta* **59**, 4889–4904.

Prahl F. G., Ertel J. R., Goñi M. A., Sparrow M. A. and Eversmeyer B. (1994) Terrestrial organic carbon contributions to sediments on the Washington margin. *Geochim. Cosmochim. Acta* **58**, 3035–3048.

Redfield A. C. (1934). *On the proportions of organic derivatives in sea water-their relation to the composition of the plankton, 176–192. James Johnstone Memorial Volume*. *Liverpool Univ. Press*, *Liverpool*.

Redfield A. C. (1958) The biological control of chemical factors in the environment. *Am. Sci.* **46**, 205–221.

Rudolphi A., Tschech A. and Fuchs G. (1991) Anaerobic degradation of cresols by denitrifying bacteria. *Arch. Microbiol.* **155**, 238–248.

Rütters H., Sass H., Cypionka H. and Rullkötter J. (2001) Monoalkylether phospholipids in the sulfate-reducing bacteria *Desulfosarcina variabilis* and *Desulforhabdus amnigenus*. *Arch. Microbiol.* **176**, 435–442.

Schmidt M. W. I. and Noack A. G. (2000) Black carbon in soils and sediments: analysis, distribution, implications, and current challenges. *Global Biogeochem. Cycles* **14**, 777–793.

Simoneit B. R. T. (2002) Biomass burning – a review of organic tracers for smoke from incomplete combustion. *Appl. Geochem.* **17**, 129–162.

Sinninghe Damste J. S. and De Leeuw J. W. (1990) Analysis, structure and geochemical significance of organically-bound sulphur in the geosphere: state of the art and future research. *Org. Geochem.* **16**, 1077–1101.

Sleighter R. L. and Hatcher P. G. (2008) Molecular characterization of dissolved organic matter (DOM) along a river to ocean transect of the lower Chesapeake Bay by ultrahigh resolution electrospray ionization Fourier transform ion cyclotron resonance mass spectrometry. *Mar. Chem.* **110**, 140–152.

Stenson A. C., Marshall A. G. and Cooper W. T. (2003) Exact masses and chemical formulas of individual suwannee river fulvic acids from ultrahigh resolution electrospray ionization fourier transform ion cyclotron resonance mass spectra. *Anal. Chem.* **75**, 1275–1284.

Taylor J. and Parkes R. J. (1983) The cellular fatty acids of the sulphate-reducing bacteria, *Desulfobacter* sp., *Desulfobulbus* sp. and *Desulfovibrio desulfuricans*. *J. Gen. Microbiol.* **129**, 3303–3309.

Tien M. and Kirk T. K. (1983) Lignin-degrading enzyme from the hymenomycete phanerochaete chrysosporium burds. *Science* **221**, 661–663.

Tremblay L. B., Dittmar T., Marshall A. G., Cooper W. J. and Cooper W. T. (2007) Molecular characterization of dissolved organic matter in a North Brazilian mangrove porewater and mangrove-fringed estuaries by ultrahigh resolution Fourier transform-ion cyclotron resonance mass spectrometry and excitation/emission spectroscopy. *Mar. Chem.* **105**, 15–29.

Tryon M., Brown K., Dorman L. and Sauter A. (2001) A new benthic aqueous flux meter for very low to moderate discharge rates. *Deep Sea Res. I Oceanogr. Res. Pap.* **48**, 2121–2146.

Verdugo P., Alldredge A. L., Azam F., Kirchman D. L., Passow U. and Santschi P. H. (2004) The oceanic gel phase: a bridge in the DOM-POM continuum. *Mar. Chem.* **92**, 67–85.

Vitorino J., Oliveira A., Jouanneau J. M. and Drago T. (2002a) Winter dynamics on the northern Portuguese shelf. Part 1: physical processes. *Prog. Oceanogr.* **52**, 129–153.

Vitorino J., Oliveira A., Jouanneau J. M. and Drago T. (2002b) Winter dynamics on the northern Portuguese shelf. Part 2: bottom boundary layers and sediment dispersal. *Prog. Oceanogr.* **52**, 155–170.

Volkman J. K., Revill A. T., Holdsworth D. G. and Fredericks D. (2008) Organic matter sources in an enclosed coastal inlet assessed using lipid biomarkers and stable isotopes. *Org. Geochem.* **39**, 689–710.

Wakeham S. G., Sinninghe Damsté J. S., Kohnen M. E. L. and De Leeuw J. W. (1995) Organic sulfur compounds formed during early diagenesis in Black Sea sediments. *Geochim. Cosmochim. Acta* **59**, 521–533.

Waterson E. J. and Canuel E. A. (2008) Sources of sedimentary organic matter in the Mississippi River and adjacent Gulf of Mexico as revealed by lipid biomarker and [delta]13CTOC analyses. *Org. Geochem.* **39**, 422–439.

White H. K., Reddy C. M. and Eglinton T. I. (2007) Relationships between carbon isotopic composition and mode of binding of natural organic matter in selected marine sediments. *Org. Geochem.* **38**, 1824–1837.

Willmann G. and Fakoussa R. M. (1997) Biological bleaching of water-soluble coal macromolecules by a basidiomycete strain. *Appl. Microbiol. Biotechnol.* **47**, 95–101.

Wu Z., Rodgers R. P. and Marshall A. G. (2004) Two- and three-dimensional van Krevelen diagrams: a graphical analysis complementary to the Kendrick mass plot for sorting elemental compositions of complex organic mixtures based on ultrahigh-resolution broadband Fourier transform ion cyclotron resonance mass measurements. *Anal. Chem.* **76**, 2511–2516.

Yoshinaga M. Y., Sumida P. Y. G. and Wakeham S. G. (2008) Lipid biomarkers in surface sediments from an unusual coastal upwelling area from the SW Atlantic Ocean. *Org. Geochem.* **39**, 1385–1399.

Associate editor: H. Rodger Harvey